UMENTATION PAGE

AD-A268 101

2. REPORT DATE	3 REPORT TYPE AND DATES COVERED
August 1993	THESIS/DISSERTATION

4. TITLE AND SUBTITLE	5. FUNDING NUMBERS
Forecasting The Ducting Of Electromagnetic Waves On The Mesoscake	

6 AUTHOR(S)

Lt Scott Phillip Simcox

7. PERFORMING ORGANIZATION NAME(S) AND ADDRESS(ES)	8 PERFORMING ORGANIZATION REPORT NUMBER
AFIT Student Attending: Pennsylvania State University	AFIT/CI/CIA- 93-122

9 SPONSORING MONITORING AGENCY NAME(S) AND ADDRESS(ES)	10. SPONSORING MONITORING AGENCY REPORT NUMBER
DEPARTMENT OF THE AIR FORCE AFIT/CI 2950 P STREET WRIGHT-PATTERSON AFB OH 45433-7765	

11. SUPPLEMENTARY NOTES

12a DISTRIBUTION AVAILABILITY STATEMENT	12b DISTRIBUTION CODE
Approved for Public Release IAW 190-1 Distribution Unlimited MICHAEL M. BRICKER, SMSgt, USAF Chief Administration	

13. ABSTRACT (Maximum 200 words)

DTIC
ELECTE
AUG 17 1993
S A D

93-18998

14 SUBJECT TERMS	15 NUMBER OF PAGES
	74
	16 PRICE CODE

17. SECURITY CLASSIFICATION OF REPORT	18 SECURITY CLASSIFICATION OF THIS PAGE	19 SECURITY CLASSIFICATION OF ABSTRACT	20 LIMITATION OF ABSTRACT

The Pennsylvania State University

The Graduate School

Department of Meteorology

93-122

FORECASTING THE DUCTING OF

ELECTROMAGNETIC WAVES ON THE MESOSCALE

A Thesis in

Meteorology

by

Scott Phillip Simcox

Submitted in Partial Fulfillment
of the Requirements
for the Degree of

Master of Science

August 1993

I grant The Pennsylvania State University the nonexclusive right to use this work for the University's own purposes and to make single copies of the work available to the public on a not-for-profit basis if copies are not otherwise available.

Scott Phillip Simcox

Scott Phillip Simcox

We approve the thesis of Scott Phillip Simcox.

Date of Signature

Hampton N. Shirer (signature)   5/21/93

Hampton N. Shirer

Associate Professor of Meteorology

Thesis Co-Adviser

Dennis W. Thomson (signature)   21 May 93

Dennis W. Thomson

Professor of Meteorology

Head of the Department of Meteorology

Thesis Co-Adviser

John L. Spiesberger (signature)   26 May 93

John L. Spiesberger

Associate Professor of Meteorology

ABSTRACT

Ducting of electromagnetic waves in the lower troposphere can have a significant impact on radar coverage. However, despite the importance of identifying ducting conditions, operational forecasts of these conditions are still based on a primitive, single-station approach. Single-station ducting analyses are available operationally through the Navy's Integrated Refractive Effects Prediction System (IREPS) software. This software can provide a satisfactory point analysis of ducting conditions, but significant spatial and temporal variations of ducting in the atmosphere can also seriously limit the utility of the output. By combining IREPS with mesoscale model output, however, there is the opportunity for significant improvement in the predictability of ducting conditions.

Subsidence inversions are a primary cause of atmospheric ducting. These inversions are common during the summer season over the west coast of the United States, particularly west-central California. Fortunately, they can be effectively modeled because they are generally very strong and quite persistent. In this thesis, a study of the predictability of inversion-generated ducting conditions over west-central California is conducted by combining output from the Penn State/NCAR non-hydrostatic mesoscale modeling system (MM5) with the IREPS ducting analysis software.

This combined modeling approach is shown to be successful in representing the levels at which ducting should occur, particularly in the morning. It also effectively represents regional trends in the ducting strength over west-central California for up to 24 hours. However, MM5 is

not as successful at representing the strength of the ducting conditions because of its relatively coarse vertical resolution near the altitude of the subsidence inversion. Also, MM5 is not able to reproduce the strong vertical gradients of temperature and moisture over the Pacific Ocean. This result is caused primarily by the poor representation of stratocumulus clouds that often cap the marine boundary layer over the eastern Pacific.

TABLE OF CONTENTS

TABLE OF CONTENTS (continued)

LIST OF FIGURES

LIST OF FIGURES (continued)

LIST OF FIGURES (continued)

LIST OF TABLES

LIST OF TABLES (continued)

ACKNOWLEDGEMENTS

Many people have contributed to the successful completion of this thesis. These people include my family, the Penn State Meteorology Department faculty, the NWP group at Penn State, AFIT personnel, and my fellow AFIT students. Among these, there are several people to whom I would like to extend special thanks.

My beautiful wife Lori has been supportive throughout this endeavor. She has provided me with more love, encouragement, friendship, and companionship than I could ever have imagined or hoped for. Also, she provided much-needed help by writing a program that produced formatted sounding data from model output. She further aided my research by manually entering some of that data into the IREPS software. My love, respect, and gratitude for this wonderful person knows no bounds.

Dr. Hampton N. Shirer is an excellent teacher, adviser, and editor. Even though the subject of this thesis is not his primary research area, he was still able to provide many valuable insights that gave me a better understanding of this topic. I continually gained self-confidence and inspiration through his motivation and his confidence in my abilities. His willingness to meet with me frequently and on short notice and his attention to every detail in the editing process vastly improved the quality of this thesis.

Dr. Dennis Thomson suggested this research after I wrote a paper that discussed the influence of sea breeze circulations on the refractivity of the lower troposphere for his atmospheric remote sensing course.

xiv

Without his input and his strong interest in this subject, this thesis would never have begun. His periodic reviews of my progress on the thesis and the suggestions that came from these meetings were very helpful. I also thank Dr. John Spiesberger for his thoughtful suggestions during the preparation of the thesis.

There were several people in the NWP group at Penn State who went out of their way to help me. Dr. Mercedes Lakhtakia responded quickly to my many requests for data. Scott Williams provided valuable help in obtaining satellite photographs and creating figures for presentation in the thesis. Dr. Dave Stauffer also took time out of his schedule to discuss the Penn State/NCAR mesoscale model.

Finally, I would like to thank the U.S. Air Force for giving me the opportunity to pursue a master's degree in meteorology at Penn State.

Chapter 1

INTRODUCTION

Ducting of electromagnetic waves in the lower troposphere is a form of anomalous propagation that can have a significant impact on radar coverage over a wide area (Bean and Dutton 1968, p. 132). Ducting in the lower troposphere is caused primarily by strong vertical gradients of temperature, water vapor, or a combination of both. Specifically, ducting can cause errors in a radar measurement of aircraft range and height, enhancing coverage at some altitudes while creating large areas of no coverage at other altitudes.

Atmospheric inversions are a frequent cause of ducting conditions in the lower troposphere. The combination of existing operational software with advanced mesoscale meteorological models capable of detecting strong inversions could provide some predictability of ducting conditions. Such predictive capability provides important and useful information to radar controllers, pilots and military commanders.

1.1. Forecasting Atmospheric Ducts

The effects of ducting on radar were commonly observed by the author at the Southeast Air Defense Sector (SEADS), Tyndall AFB, Florida over a period of several years from 1989 to 1991. In one case, a large oil tanker was observed on a SEADS air-search radar apparently flying toward

the South Carolina coast at a speed of approximately 30 knots. In other cases, significant numbers of helicopters ferrying supplies and personnel to oil rigs off the Louisiana coast at low altitudes would appear on radar for a period of time even though they were flying at altitudes well below the expected coverage of the radar. In contrast, while coverage is enhanced at the lowest altitudes, at the same time it may be nonexistent over a large area at altitudes just above the ducts.

Software that attempts to assess the effects of atmospheric ducting conditions on radar systems has been developed and distributed for operational use (Patterson 1988). This software, the Navy's Integrated Refractive Effects Prediction System (IREPS), uses an atmospheric sounding to determine whether ducting conditions are present over a station.

Unfortunately, many operational forecasters are unfamiliar with the effects of ducting on radars and the IREPS software, and hence, forecasts for the cases described above merely involved a qualitative description of the ducting conditions. This description only noted that ducting conditions were favorable during the next several days. After these events, analyses of nearby soundings using IREPS software showed that ducting conditions were present near the locations and times of the aforementioned events.

Clearly, methods must be found to utilize IREPS software more effectively. Integrating IREPS software into a mesoscale model could provide important information to radar controllers, pilots, and military commanders. For example, from contours of the refractivity gradient values, certain patterns and trends in the strength and spatial extent of the ducting conditions will become apparent. Radar controllers could use a ducting forecast of this type to determine in advance whether anomalous propagation

conditions are caused by atmospheric conditions or radar malfunctions. More significantly, controllers would be aware of possible radar holes, which are regions in which coverage would be lost or severely degraded because of the ducting conditions. Commanders could use improved ducting forecasts to aid the deployment of airborne radars into regions where surface radars might be experiencing ducting-induced degradation in coverage. In an offensive mode, pilots could use forecasts for mission planning to determine the best flight path for radar avoidance.

1.2. The Subsidence Inversion

Atmospheric inversions are one of the primary causes of ducting in the lower troposphere. In particular, subsidence inversions can create the strong vertical gradients of temperature and water vapor necessary to produce ducting conditions. Fortunately, subsidence inversions are also the simplest of inversions to represent in mesoscale models because in general, they cover a large area, and are very strong and very persistent. Thus, if a subsidence inversion can be identified in the atmosphere, then mesoscale model output with a reasonable vertical resolution can be combined with IREPS software to examine the predictability of ducting conditions. This is the premise on which the research in this thesis is based.

The eastern edge of a large ocean basin is a prime location for the formation and maintenance of a subsidence inversion during the summer season (McIlveen 1986, p. 366). West-central California is located along the eastern boundary of the Pacific Ocean, where a strong subsidence inversion is indeed present during much of the summer (Felsch and Whitlatch 1990).

4

Thus, this area is ideal for research into using a mesoscale model to improve the predictability of atmospheric ducting of electromagnetic waves.

1.3. Selection of a Mesoscale Model

The next step, then, is to find a mesoscale model that has both a vertical resolution sharp enough to capture the subsidence inversion and a horizontal resolution fine enough to resolve the large geographical features of the west-central California region. The Penn State/NCAR nonhydrostatic Mesoscale Modeling System (MM5) was available for use in this project (Seaman et al. 1992). The model has a nested grid, with horizontal resolutions of 30, 12, and 4 km. The 30 km grid is too coarse for a study of ducting predictability near the west coast because it is too coarse to effectively resolve the Coastal Ranges of west-central California. The 4 km grid resolves the Coastal Ranges well, but does not include the entire region of interest. For these reasons, the 12 km grid was chosen as a compromise between spatial coverage and horizontal resolution. Vertically, the model contains 30 layers, with a variable resolution that is finest near the surface. The vertical resolution is about 8 mb near the surface, and approximately 14 mb near 1000 m above ground level, where the subsidence inversion tends to occur. Although this is somewhat coarse for representing inversions, this resolution should still capture the strength and depth of a west-central California subsidence inversion well enough to provide meaningful results.

Fortunately, an MM5 simulation that includes west-central California was run as part of the SJVAQS/AUSPEX Regional Modeling Adaptation Project (SARMAP) (Seaman et al. 1992). This SARMAP simulation included

the August 2-3, 1990 period, throughout which a strong subsidence inversion existed over most of west-central California. Because of the strong subsidence inversion, and because the 12 km horizontal resolution is a good compromise between the horizontal spatial coverage and the grid resolution, the MM5 SARMAP simulation was selected for this study of atmospheric ducting.

An advantage of using MM5 is that forecasts could be made at frequent intervals. However, to calibrate the model with the observations, the model hours chosen for this study are the initial, 12, and 24 hour simulation times. These times correspond to 12 UTC, August 2, 1990, and 00 UTC and 12 UTC, August 3, 1990, respectively. Soundings for these times at Oakland and Vandenberg AFB are examined to determine the inversion strength and depth. Then data from both stations are entered into the IREPS software to find the strength and depth of the associated atmospheric duct. Next, model output for the grid columns closest to these locations are examined and compared with the observations in order to calibrate the model. Finally, the strength of the refractivity gradient is calculated at various locations throughout west-central California.

Chapter 2

REFRACTIVITY IN THE LOWER TROPOSPHERE

Anomalous propagation of electromagnetic waves, e.g. radar and radio waves, in the lower troposphere occurs when there are strong vertical gradients of refractivity. One type of anomalous propagation is ducting. Ducting is a term applied to an atmospheric region in which electromagnetic waves may be confined by unusually large vertical refractivity gradients. It is generally found in areas where there is a rapid decrease with height of water vapor, a rapid increase with height of temperature, or a combination of the two. The latter case is often found in the atmosphere in a subsidence or radiation inversion. Hence, ducting of electromagnetic waves might be expected when inversions are present in the lower troposphere. Further information on the causes of ducting in the lower troposphere is available in Bean and Dutton (1968).

Software is currently available that can determine whether and at what heights inversions may cause ducting conditions (Patterson 1988). Also, mesoscale models now exist that might be able to predict the moderate to strong inversions that are conducive to ducting. One area where inversions are almost a permanent feature is west-central California, where a synoptic-scale subsidence inversion is present throughout most of the summer (Felsch and Whitlatch 1990). Fortunately, a mesoscale model

simulation already exists for this area and season (Seaman et al. 1992). Thus, by combining one of the best available mesoscale models with ducting analysis software, a determination can be made as to the predictability of ducting events up to 24 hours in advance.

2.1. Refractivity and Ducting

Refractivity is the bending of waves owing to differing densities and molecular species within a medium. The index of refraction n is defined as the ratio of the velocity c of an electromagnetic wave in a vacuum to the velocity v of an electromagnetic wave in a medium. To simplify calculations, a radio refractivity N is introduced, where

$$N = (n-1) \times 10^6 \tag{2.1}$$

The refractivity of a radio wave varies from point to point in the lower troposphere because it is highly dependent on density. The density of the lower troposphere is, in turn, dependent on water vapor, pressure, and temperature. The dependence on water vapor is particularly significant because of the polarizability of water molecules. The molecules quickly adjust to changing electric fields, thereby increasing the refractivity of the radio waves. This density and polarization dependence can be quantified using the Smith-Weintraub relation

$$N = \frac{77.6}{T}(p + 4810 \times \frac{e}{T}) \tag{2.2}$$

where T is the temperature in K, p is the atmospheric pressure in mb, and e is the partial pressure of water vapor in mb; values are thus given by (2.2) in "N-units" (Bean and Dutton 1968).

Normally, the value of the vertical gradient dN/dz of refractivity in the troposphere is about -40 N-units per km. If the vertical gradient of refractivity is positive, then subrefractive conditions are present (Figure 2.1). In the atmosphere, this condition is generally found near the surface in very dry regions where surface heating is strong. Electromagnetic waves propagate away from the surface of the Earth, and low level radar coverage is degraded. When the vertical gradient of refractivity is between -79 and -157 N units per km, a superrefractive condition is present. The value of -157 N-units per km represents the bending of electromagnetic waves along a path parallel to the surface of the Earth. Ducting of electromagnetic waves in the lower troposphere occurs when the magnitude of the vertical gradient of refractivity is less than a critical value, -157 N units/km (Bean and Dutton 1968, p. 146). In this case, the electromagnetic waves are said to be trapped, because their curvature by the atmosphere is greater than the curvature of the earth. For example, waves entering the ducting layer from below will be reflected back to the base of the duct, then reflected upward again. This situation is analogous to a wave guide, except that the duct boundaries are neither permanent nor free from energy losses.
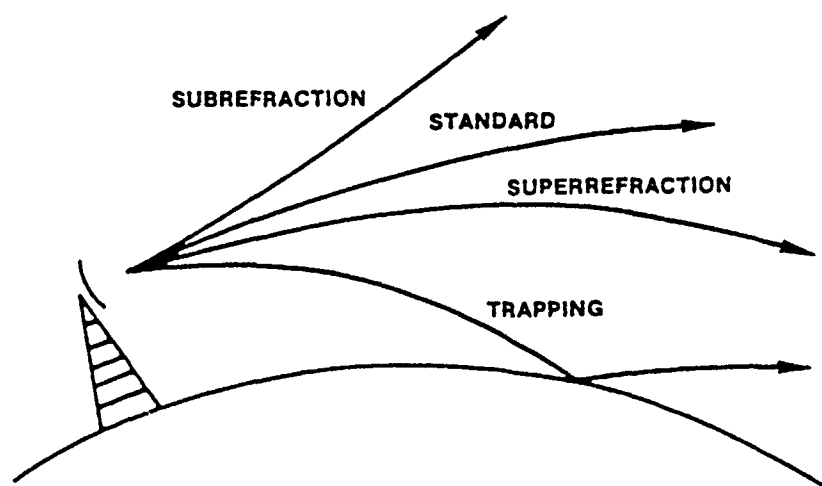
Figure 2.1. Wave paths for various refractive conditions (from Patterson 1988).

2.2. Meteorological Situations Conducive to Duct Formation

There are several meteorological situations that can cause the rapid vertical variations in water vapor concentration and temperature necessary for trapping. These atmospheric conditions, which enhance the formation of inversions and ducting conditions, are radiational cooling, synoptic-scale subsidence, and sea-land breeze circulations. A synoptic-scale inversion can form through radiational cooling or large-scale subsidence. Inversions that form by radiational cooling can sometimes result in ducting conditions, especially when there has been little mixing of low-level moist air during the day. Moisture would then be trapped in the lowest levels of the atmosphere, with rapid drying above the inversion cap. A more likely and longer lasting scenario is the existence of large-scale subsidence in the atmosphere. As air in a high pressure cell sinks, it warms and dries, providing a strong cap to the mixed layer. If the mixed layer originates from a marine environment, with cool moist air, then the conditions are optimal for the formation of atmospheric ducts.

The sea-land breeze circulation found in coastal areas also contributes to the formation and maintenance of ducting conditions. During the day, the sea breeze circulation produces subsidence aloft over coastal waters (Figure 2.2). The air advected aloft from the land mass over the water is warm and dry, strengthening the strong cap to the marine layer; the resulting inversion can have the steep gradient of temperature and water vapor concentration necessary for ducting conditions. At night, the land breeze provides subsidence over the coastal land mass. This, combined with radiational cooling of the land mass, may also provide gradients steep enough to
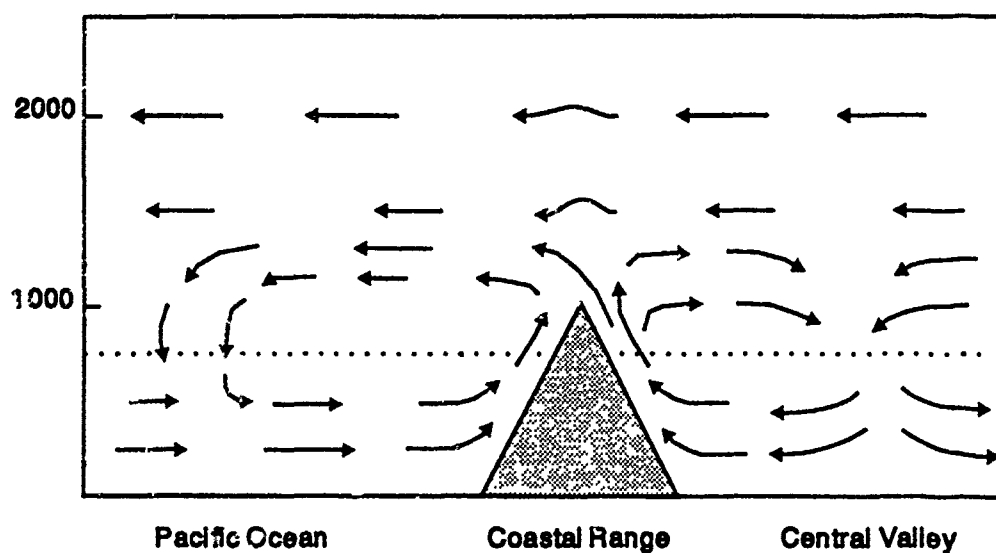
Figure 2.2. Mesoscale circulations present during the day over west-central California. Altitude is in m. The base of the synoptic-scale subsidence inversion is denoted by the dotted line, but the moist marine boundary layer does not penetrate inland beyond the Coastal Range. A sea breeze circulation is on the west side of the Coastal Range, while a mountain-valley circulation is on the east side.

generate ducting conditions close to the ground. However, the air advected aloft from over the water is moist, so this situation is not as conducive to the creation of ducting conditions as the sea breeze. Nevertheless, ducting is expected aloft over the water during the day, and either at the surface or aloft over land at night.

Another condition that can form an atmospheric duct is the strong, continuous, and turbulent moisture flux between the ocean and the atmosphere. The air a few tens of meters above an ocean surface carries large amounts of moisture, with a rapid decrease in moisture content just above. The moisture gradient is large enough to form what is known as an evaporative duct. This duct is a persistent feature over many of the world's oceans, but the strength and depth of it varies considerably in both the horizontal and the vertical.

The coast of the western United States is an ideal location for the study of ducting conditions because all of the atmospheric processes described above are present, especially in the summer. However, the complex terrain along the coast and the associated mesoscale and microscale processes modifies the ducting conditions that would be created by the sea-land breeze circulations and the synoptic-scale subsidence. Strong ducting conditions aloft would be observed during the day over coastal land areas, because warm air flowing over the mountains from the east and the synoptic-scale subsidence should provide a strong, stable cap. Over the inland areas, warm and dry air at the surface would keep the moisture and temperature gradients too small at the level of the subsidence inversion for ducting to occur.

2.3. The Geography and Weather of West-Central California

The geography of west-central California is rugged. The Coastal
Range extends from the Diablo and Santa Lucia Mountains in the north and
central sections to the San Rafael, Santa Ynez, and Tehachapi Mountains in
the south (Figure 2.3). To the east of the Coastal Range is the Central
Valley, which extends from north to south through the region and is
approximately 40 miles wide. At the northern end of this area, the
Sacramento River basin provides the only sea-level access to the Central
Valley. The Coastal Range is cut by several passes throughout the region,
including the Pacheco, Panoche, and Cottonwood passes in the northern and
central sections and the Tehachapi pass in the southern section.
Additionally, the Salinas Valley separates the Santa Lucia and Gabilan
Mountains southeast of Monterey. These topographic features appear to
have a significant effect on the variation of ducting conditions throughout
west-central California.

The weather conditions present during the summer season in west-
central California are a result of its geographic location and the topography
of the area. California is located on the eastern side of the Pacific Ocean. It
is commonly observed (McIlveen 1986, p. 363) that the synoptic weather
pattern over eastern coasts of large ocean basins during the summer season
is dominated by high pressure at all levels of the atmosphere. The mesoscale
circulations are a result of the diurnal temperature fluctuations of the land
mass, and the rugged terrain of the region. Along the immediate coast, a sea-
land breeze circulation forms due to temperature differences between the
water and the land. Mountain-valley circulations also develop because of
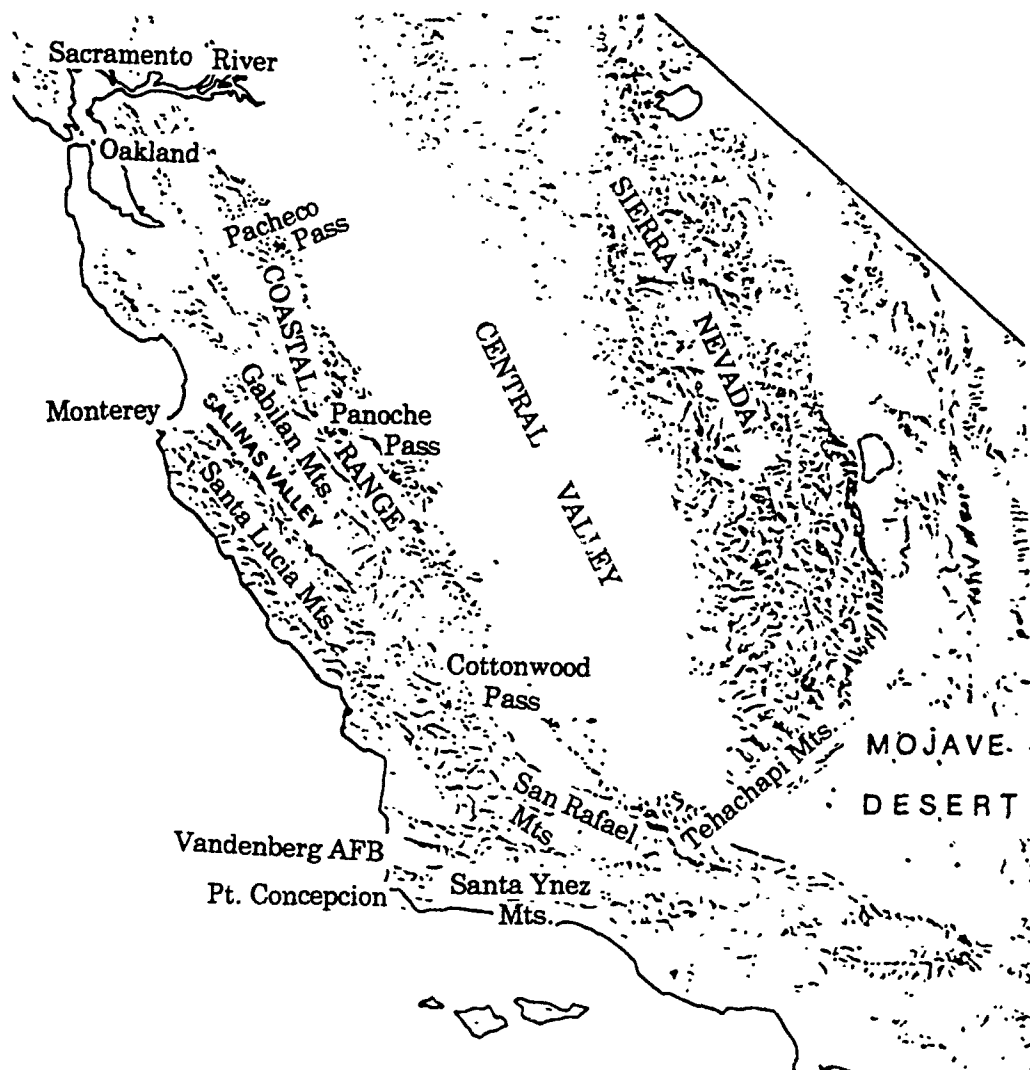
Figure 2.3. Geography of west-central California. Oakland is on the eastern shore of San Francisco Bay. Vandenberg AFB is on the coast, just north of Point Concepcion (from Hornbeck 1983).

temperature differences between high and low terrain. These weather conditions, all of which were present during the August 2-3, 1990 period, can combine to produce strong inversions and ducting conditions throughout west-central California. For example, refractivity gradients of -1340 N units/km over Oakland and -1500 N units/km over Vandenberg Air Force Base were calculated by IREPS based on sounding data on 12 UTC, August 3, 1990. Although the magnitudes of these values may be artificially high due to evaporative cooling errors in the radiosonde equipment (Section 3.1), it is likely that corrected refractivity gradient magnitudes would still greatly exceed the critical value of 157 N units/km required for ducting.

High pressure centered over the eastern Pacific Ocean dominates the synoptic weather pattern for a large part of the August 2-3, 1990 period. The surface analysis for 00 UTC, August 3, 1990 is shown in Figure 2.4 and typifies the overall synoptic pattern for the period of the simulation. High pressure centered over the eastern North Pacific Ocean produces a clockwise wind pattern, with northerly winds along the California coast. These northerly winds enhance the upwelling of cold water which, in turn, further stabilizes the atmospheric marine boundary layer. Aloft, the high pressure system produces synoptic-scale subsidence. This warms and dries the air mass immediately above the stable marine layer through adiabatic compression. These processes combine to form an extremely strong and persistent synoptic-scale subsidence inversion.

Mesoscale processes serve to regionally strengthen or weaken the synoptic-scale subsidence inversion. These processes are produced by the large temperature contrast between the cool water and the hot, dry Central Valley, as well as other geographic features of the area. The differences in
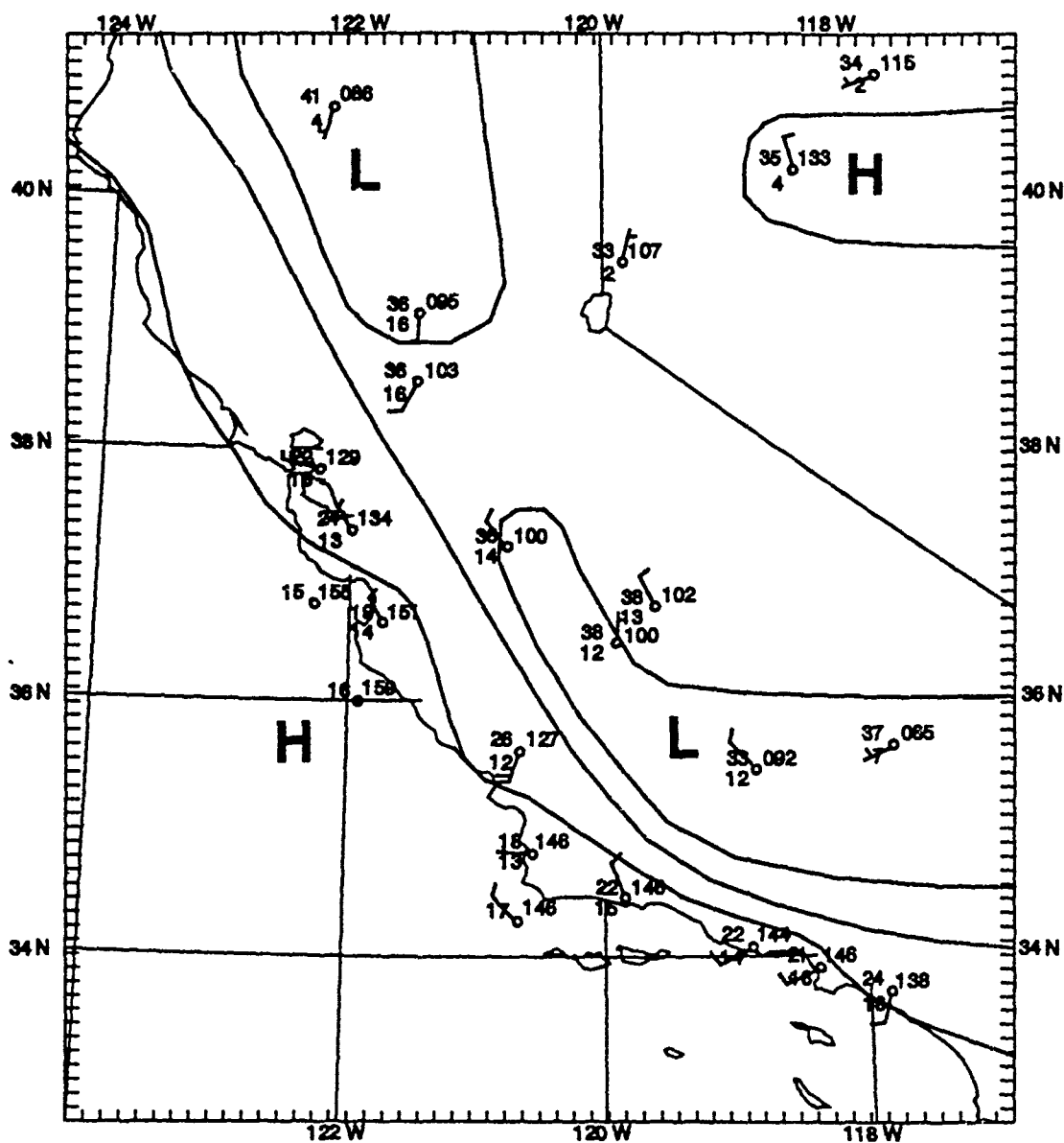
Figure 2.4. Surface analysis of weather conditions on 00 UTC, August 3, 1990. Low pressure, induced by surface heating, extends from the Mojave Desert through the Central Valley. Higher surface pressures exist offshore, where the large heat capacity of water prevents strong daytime heating of the surface.

temperature between the ocean water and the land create a sea-land breeze circulation over most of the coastal region west of the Coastal Range (Figure 2.2). Inland, a mountain-valley circulation develops over the Central Valley and the east slopes of the Coastal Range. During the day, strong heating over the Central Valley forms a heat trough. This tightens the surface pressure gradient, and intensifies the onshore surface flow west of the Coastal Range. West of the Coastal Range, the synoptic-scale subsidence inversion is strengthened during the day as hot and dry air cascades westward over the mountains. However, some of the air flows back into the heat trough and descends, further strengthening the synoptic-scale subsidence inversion over the Central Valley. Although the inversion strengthens, this does not necessarily imply increased refractivity gradients, because the air below the inversion is generally dry.

During the overnight hours, a weak land breeze circulation develops along most of the coastal areas. Offshore flow at the surface is weak. The return flow aloft is difficult to detect because it is embedded in the synoptic-scale northwesterly flow. However, descending air in the land breeze circulation and radiational cooling appears to strengthen the synoptic-scale subsidence inversion and thus, provides conditions optimal for duct formation. Meanwhile, the inland areas from the Coastal Range eastward experience a circulation down the mountains and into the valley. Upward vertical motion from the valley floor counters the synoptic-scale subsidence. This may inhibit nocturnal duct formation over the Central Valley.

The geography of west-central California effectively prevents the penetration of the cool and moist marine air into the Central Valley, except through the Sacramento River Valley and through several of the mountain

passes. The flow up the Sacramento River Valley is particularly strong, with surface winds sustained at over 20 knots during the afternoon and 15 knots at night. This funneling of the cool moist air up the river valley occurs there because it is the only significant break in the Coastal Range at sea level.

In summary, the synoptic weather pattern over west-central California during the August 2-3, 1990 period is dominated by the high pressure system centered over the eastern Pacific Ocean. This system produces large scale subsidence over the entire area. Mesoscale processes, including sea-land breeze and mountain-valley circulations, strengthen or weaken this inversion. Inland areas west of the Coastal Range during the day, and the immediate coastal areas at night, experience the greatest enhancement of the synoptic-scale inversion and associated ducting conditions. The southern section of the Central Valley is the least likely location to experience enhanced ducting conditions no matter how strong the inversion, because there is insufficient moisture in that area.

2.4. A Software Program for Detecting Ducting Layers

The Integrated Refractive Effects Prediction System (IREPS) is a program designed to give forecasters a single-station analysis of ducting conditions based on the input of radiosonde data. The IREPS software calculates vertical refractivity gradients and provides a forecaster with radar coverage diagrams based on the atmospheric conditions recorded by a radiosonde. The program was designed and developed by the U.S. Navy, and is also used operationally by some U.S. Air Force weather units to determine the effect of atmospheric ducting on coastal surveillance radars. Sample

output from the IREPS software is shown in Figure 2.5. Further details on the capabilities, uses and limitations of the IREPS software are available in Patterson (1988). The calculation of vertical refractivity gradients and the subsequent determination of atmospheric ducts is important. However, a forecaster must be extremely careful in interpreting IREPS output not only because of the errors inherent in radiosonde data, but also those resulting from the horizontally inhomogeneous structure of the atmosphere.

Radiosonde data are also subject to errors, especially when the instrument penetrates subsidence inversions above the marine layer. As the radiosonde rises through the saturated marine layer, condensation can occur on the sensors. Thus, when the radiosonde rises into the drier air in the inversion, evaporational cooling can retard the increase in measured temperature. This slows the decrease in measured relative humidity, and hence the inversion strength is underestimated (Nash and Schmidlin 1987). Problems such as these can account for altitude errors of 35-40 m in the height of the inversion base.

Horizontal inhomogeneities call into question the representativeness of a single sounding over a wide area. This factor can seriously limit the utility of IREPS output. Differences in temperature and water vapor concentration are significant in coastal areas, especially when there is a combination of sea/land breeze circulations and large-scale subsidence. The addition of rugged coastal terrain also increases horizontal inhomogeneities. Thus, the application of IREPS in these areas is fraught with possibilities for error. However, by combining IREPS with output from a mesoscale model, it is hoped that the problems of horizontal inhomogeneity can be effectively alleviated.
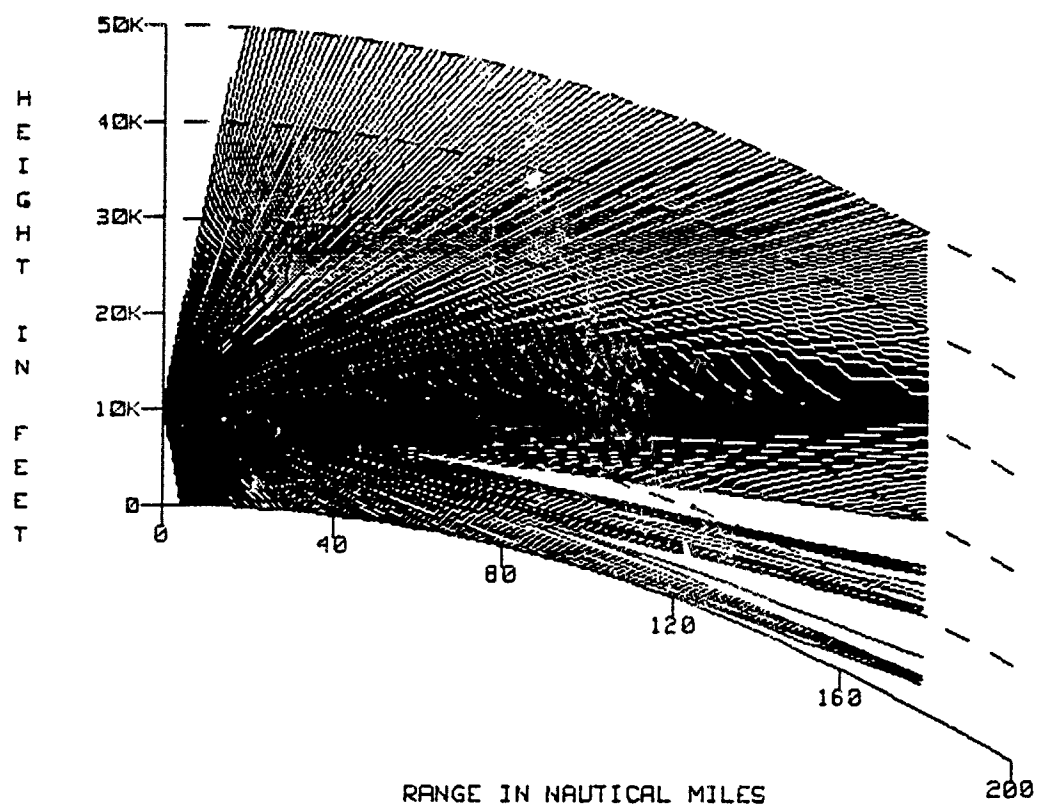
Figure 2.5. Sample output from IREPS for an irborne radar over San Diego on August 7, 1987. Shaded area indicates region of radar detection; however the assumption of horizontal homogeneity limits the utility of this output (from Patterson 1988).

2.5. A Mesoscale Model for Simulating Atmospheric Processes

A simulation that can adequately capture strong temperature and water vapor gradients occurring in the complex geography of west-central California requires an extremely advanced mesoscale model. One of these models is the Penn State/NCAR MM5 nonhydrostatic mesoscale modeling system. The simulation for August 2-3, 1990 was originally run as part of the SJVAQS/AUSPEX Regional Modeling Adaptation Project (SARMAP). This simulation was conducted to study the processes that lead to high ozone concentrations in the San Joaquin Valley (Seaman et al. 1992). Data for the simulation included National Weather Service observations, special SJVAQS/AUSPEX soundings, profilers, acoustic sounders, and surface observations.

The model uses three nested domains of horizontal resolution 36, 12, and 4 km, with 30 layers in the vertical for each. Output from the 12 km grid is used for the results given in Chapter 3. Of the 30 vertical layers, the lowest layer is 35 m above ground level, and 10 are in the lowest 1500 m of the atmosphere. Although this vertical resolution is still somewhat coarse for detecting all ducting conditions, it is fine enough to resolve the strong synoptic-scale subsidence present during the study. The planetary boundary layer is simulated using a medium resolution Blackadar scheme (Seaman et al. 1992). It has four stability regimes; stable, damped mechanical turbulence, neutral, and unstable. Another important aspect of the model is its use of four-dimensional data assimilation (FDDA). This process uses Newtonian relaxation (nudging) to introduce observations into the model throughout the simulation to reduce the growth of numerical errors. Further

information on both the MM5 model and the SARMAP project is available in Seaman et al. (1992).

Applying model output to the IREPS software can yield a prediction of the structure and evolution of regional ducting conditions. Presently, however, ducting conditions will likely be more intense than the output will indicate, because of the relative coarseness of the vertical resolution of MM5. The objective of this thesis is to determine whether or not the combination of the Penn State/NCAR mesoscale model and the IREPS software can successfully identify the existence and location of inversions and the associated ducting conditions when these conditions are particularly strong.

Chapter 3

DUCTING CONDITIONS OVER WEST-CENTRAL CALIFORNIA

Ducting conditions were present in areas of west-central California throughout the August 2-3, 1990 period. Atmospheric soundings and IREPS analyses from two stations in west-central California show inversion and ducting layers of varying strength and altitude. It is shown in this chapter that the MM5 model output for 12 UTC, August 2, 1990, and 00 and 12 UTC, August 3, 1990 does not represent these inversion conditions well in terms of strength and altitude, because the model tends to broaden the inversions vertically. However, it is also found that the model output represents the expected diurnal trends in the inversion strength and depth throughout the entire west-central California region, and the IREPS output shows the associated strengthening or weakening of the ducting layers in various grid columns.

3.1. Observed Inversion and Ducting Conditions

There are two National Weather Service upper-air reporting stations in west-central California, at Oakland and Vandenberg AFB. Both stations are located in areas where the marine boundary layer was present throughout the entire August 2-3, 1990 period. Hence, synoptic-scale

subsidence inversions were persistent features at both stations. In this study, the bases of the inversions are defined for both observations and model grid columns to be the level above which the relative humidity decreases by more than one percent. The bases of the inversions are defined using relative humidity because of evaporative cooling problems in the radiosondes. The tops of the inversions are defined more conventionally to be the level at which there is a local maximum of temperature. Observations are entered into the IREPS software to determine the maximum refractivity gradient magnitude and the thickness of the atmospheric duct at each location and time.

It is very apparent that the radiosondes used at Oakland and Vandenberg AFB during this period were affected by evaporative cooling errors in the temperature element. For example, the 12 UTC, August 2, 1990 Vandenberg AFB sounding data indicated that the dew point temperature began to decrease rapidly at 938 mb. In fact, within 6 mb, the dew point depression fell to 30°C, the maximum depression reported on standard radiosonde reports. However, during this drastic fall in humidity, the temperature also continued to fall. This temperature decrease is most likely the result of cooling caused by rapid evaporation of water droplets from the temperature sensor of the radiosonde (Nash and Schmidlin 1987). In actuality, the temperature more likely remained constant or even increased in value.

The effect of the errors on IREPS output is to significantly increase the calculation of the refractivity gradient magnitudes. After a correction was applied to the 12 UTC, August 2, 1990 Vandenberg AFB sounding data, the maximum refractivity gradient magnitude decreased from 2215 N-units per

km to 758 N-units per km. Similar decreases in the maximum refractivity gradient magnitudes were observed in the other cases after corrections were applied. However, in no case did the corrections result in a decrease in the refractivity gradient magnitude below the 157 N-unit per km critical magnitude for ducting. Therefore, the observed data were retained with no corrections applied.

3.1.1. Inversion and Ducting Conditions at Oakland

Soundings for Oakland on 12 UTC, August 2, 1990, and on 00 and 12 UTC, August 3, 1990 are shown in Figures 3.1, 3.2 and 3.3 on Skew T-Log P diagrams. It is clear from all three figures that the boundary layer inversion is very strong and very well-defined, especially for the two morning (12 UTC) soundings. A summary of the inversion base and top, which includes the temperature and relative humidity at each level, is shown for all three soundings in Table 3.1.

The 12 UTC, August 2, 1990 sounding data show that the inversion base is at a pressure level of 948 mb, where the temperature is 12°C, and the relative humidity is 95%. The top of the inversion is at a pressure level of 916 mb, where the temperature is 28°C and the relative humidity is 14%. For this inversion, the IREPS software calculates a maximum refractivity gradient magnitude of 680 N-units per km between the 945 and 942 mb pressure levels. This value is significantly greater than the 157 N-unit per km magnitude required for ducting conditions. A summary of the pressure levels, the maximum refractivity gradient magnitude, and the thickness of the atmospheric duct is compiled in Table 3.2. It should be noted that

Figure 3.1. Skew T-Log P diagram for the 12 UTC, August 2, 1990 Oakland sounding. Pressure is in mb, temperature and dew point temperature are in °C. Winds are shown using the standard station plotting convention.

Figure 3.2. Skew T-Log P diagram for the 00 UTC, August 3, 1990 Oakland sounding. Pressure is in mb, temperature and dew point temperature are in °C. Winds are shown using the standard station plotting convention.

Figure 3.3. Skew T-Log P diagram for the 00 UTC, August 3, 1990 Oakland sounding. Pressure is in mb, temperature and dew point temperature are in °C. Winds are shown using the standard station plotting convention.

Table 3.1. Summary of the observed synoptic-scale subsidence inversion at Oakland from the soundings in Figures 3.1, 3.2, and 3.3.

		Pressure	Temperature	Relative Humidity
		(mb)	(°C)	(%)
12 UTC	Base	948	12	95
August 2, 1990	Top	916	28	14
00 UTC	Base	955	16	81
August 3, 1990	Top	915	26	22
12 UTC	Base	948	12	95
August 3, 1990	Top	916	26	14

Table 3.2. Summary of the IREPS output calculated using the three observations at
Oakland shown in Figures 3.1, 3.2, and 3.3. The pressure levels define the layers in which
the refractivity gradient magnitude is the largest. The depth of the ducting layer is given
by refractivity gradient magnitudes greater than 157 N-units per km.

	Pressure Levels	Maximum Refractivity Gradient Magnitude	Depth of Ducting Layer
	(mb)	(N-units/km)	(m)
12 UTC August 2, 1990	945-942	680	455
00 UTC August 3, 1990	939-932	360	187
12 UTC August 3, 1990	944-940	1281	476

because the data are from an early morning sounding (0400 PST), this value
would be near the expected maximum N-unit gradient for this location and
date.

Figure 3.2 shows the Skew T-Log P diagram for the 00 UTC, August
3, 1990 (1600 PST, August 2, 1990) Oakland sounding. It is seen from the
diagram that, although the inversion has weakened, it is still well-defined.
The base of the inversion has lowered in altitude to a pressure level of 955
mb. The temperature at the base has risen to 16°C, and the relative
humidity has fallen to 81% (Table 3.1). The top of the inversion has risen
slightly to a pressure level of 915 mb, where the temperature is 26°C, and the

relative humidity is 22%. Thus, the inversion has broadened vertically between the morning and afternoon soundings, while the differences in temperature and relative humidity between the base and top of the inversion have decreased.

With the broadening and weakening of the inversion between the morning and afternoon soundings, it would be expected that both the maximum refractivity gradient magnitude and the depth of the ducting layer calculated by the IREPS software would decrease. This is found to be the case, as the maximum refractivity gradient magnitude decreases to 360 N-units per km and the thickness of the duct decreases from 455 m to 187 m between the two soundings (Table 3.2). It is interesting to note that the 260 m decay in the depth of the ducting layer occurs from below. This is consistent with expectations of the diurnal variability of ducting conditions (Section 2.4). While large-scale subsidence maintains the duct from above, surface heating and the subsequent mixing of moist marine boundary layer air with warm and dry air above gradually erodes the duct from below.

The Skew T-Log P diagram for the 12 UTC, August 3, 1990 Oakland sounding is shown in Figure 3.3. It is clear that the subsidence inversion has strengthened overnight, and conditions at the base and top of the inversion are very similar to those on 12 UTC, August 2, 1990 (Figure 3.1). The base of the inversion is again at a pressure level of 948 mb, where the temperature is 12°C and the relative humidity is 95% (Table 3.1). The top of the inversion is at a pressure level of 916 mb, where the temperature is 26°C and the relative humidity is 14%. It is interesting to note that the pressure levels of the base and top of the inversion are identical to those measured 24 hours earlier. In fact, the only difference between the inversion base and top characteristics is

a decrease of 2°C in the temperature. Again, the data reflect the expected diurnal trend in the thickness and strength of the subsidence inversion.

It is noted that the subsidence inversion has a larger maximum refractivity gradient magnitude on 12 UTC, August 3, 1990 than it had 24 hours before. Table 3.2 shows that the IREPS output produces a maximum refractivity gradient magnitude of 1281 N-units per km between the 944 and 940 mb pressure level at 12 UTC, August 3, 1990. The sharp increase from that found using the 12 UTC, August 2, 1990 data is caused by a tightening of the moisture gradient within the inversion. However, despite this increase, the IREPS output shows that the depth of the ducting layer increased by only 21 m.

The soundings at Oakland clearly show the existence of a strong, well-defined subsidence inversion at all three times. However, the strength and depth of the duct are subject to variability caused by surface heating and the subsequent mixing of moist marine boundary layer air with dry air above. As expected, the inversion and associated ducting conditions decay upward from the base during the day, but build downward overnight.

3.1.2. Inversion and Ducting Conditions at Vandenberg AFB

Soundings for Vandenberg AFB on 12 UTC, August 2, 1990 and on 00 UTC and 12 UTC, August 3, 1990 are shown in Figures 3.4, 3.5, and 3.6. Because this station is on the coast and the marine boundary layer is a permanent feature there for the duration of this study, the inversion and associated ducting conditions might be expected to be very similar to those at
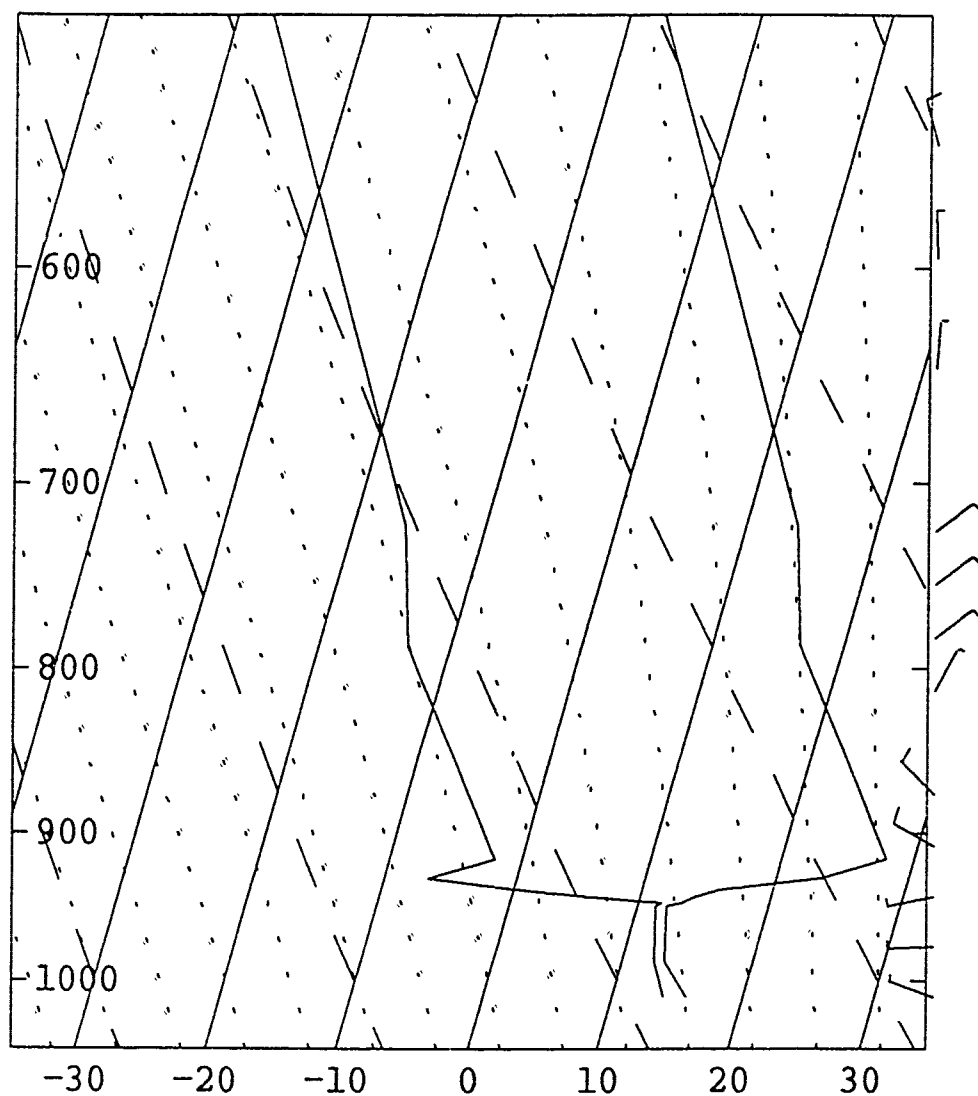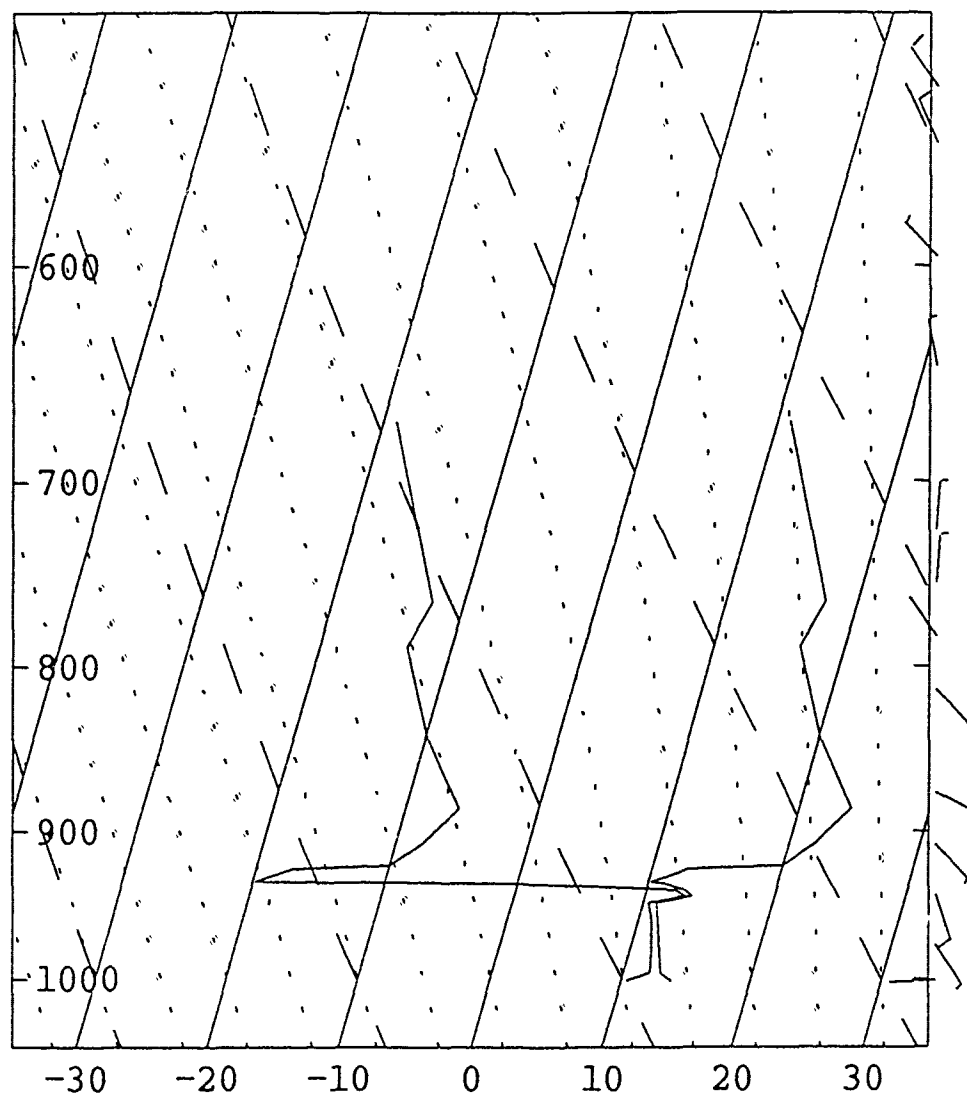
Figure 3.4. Skew T-Log P diagram for the 12 UTC, August 2, 1990 Vandenberg AFB sounding. Pressure is in mb, temperature and dew point temperature are in °C. Winds are shown using the standard station plotting convention.
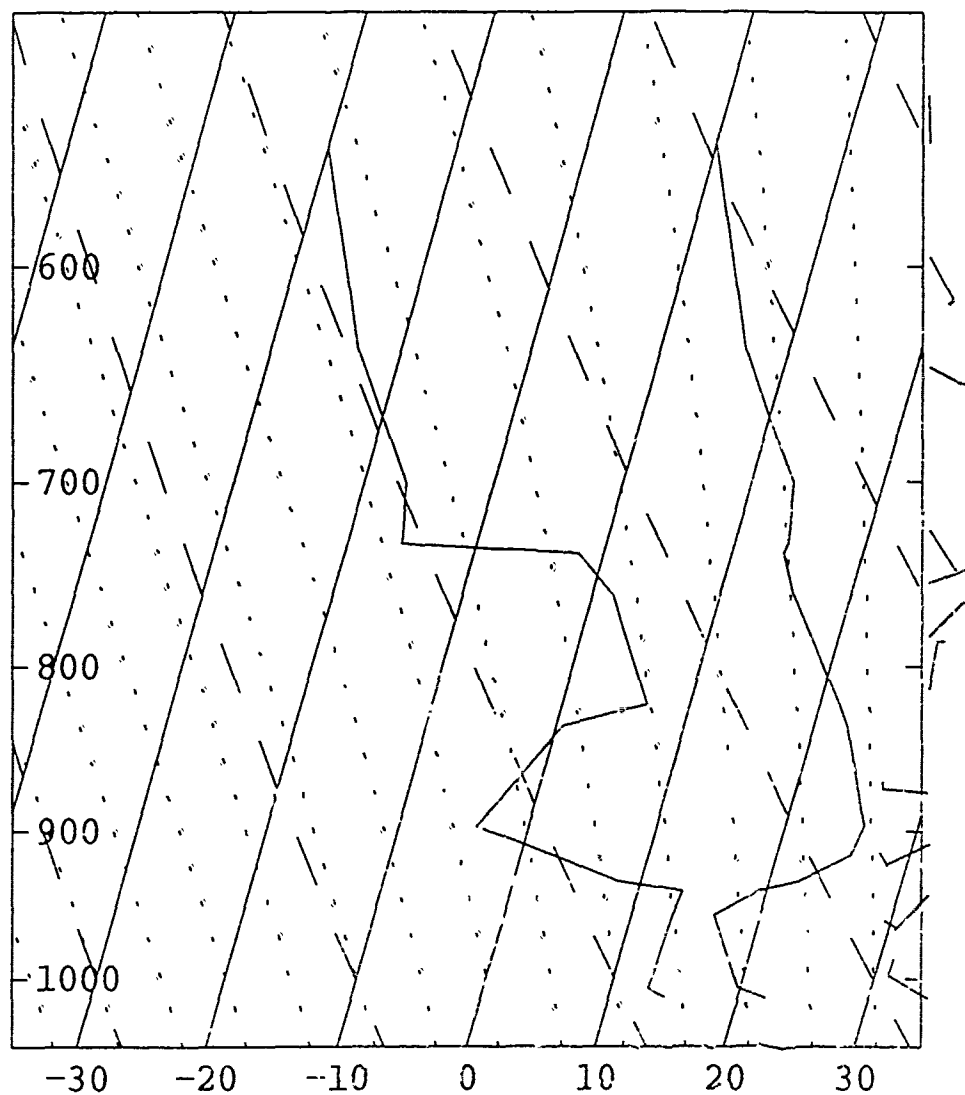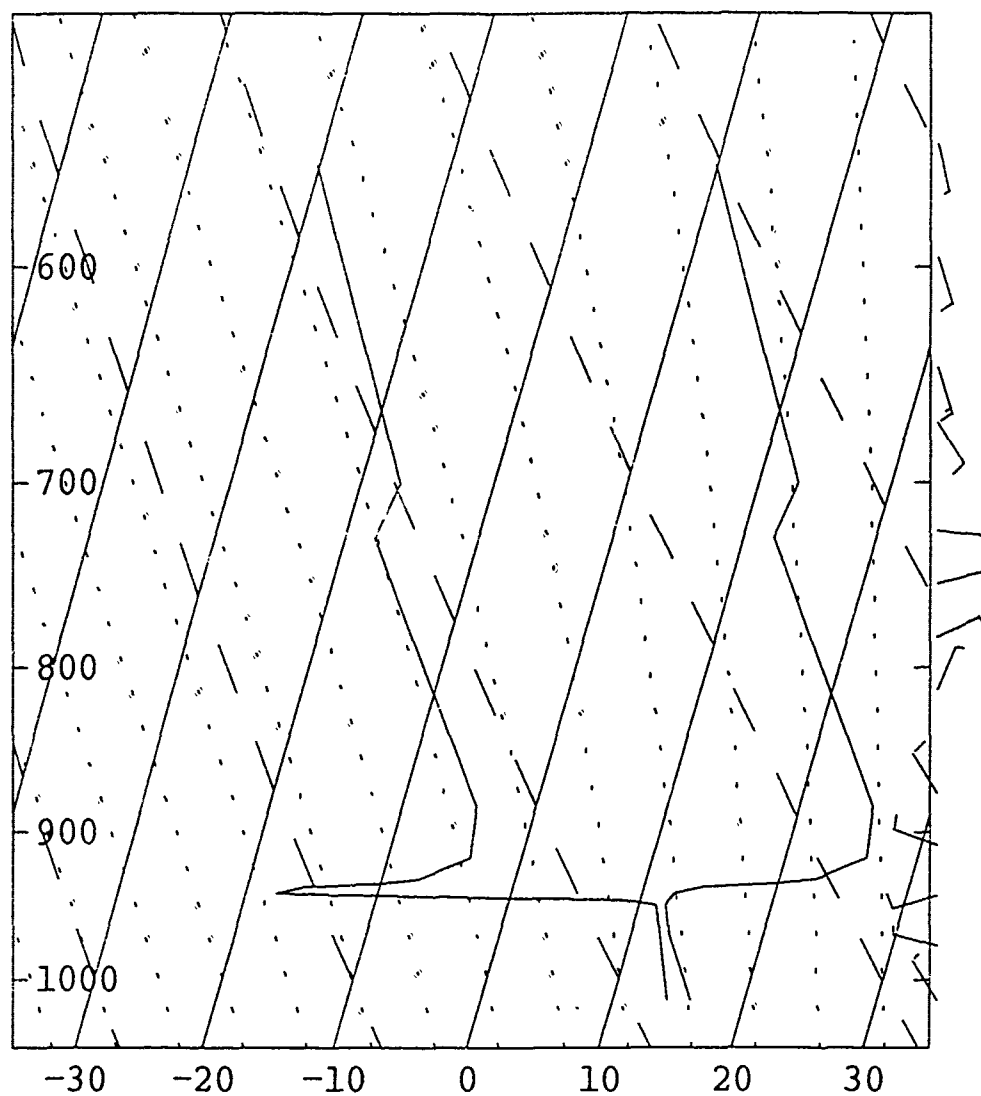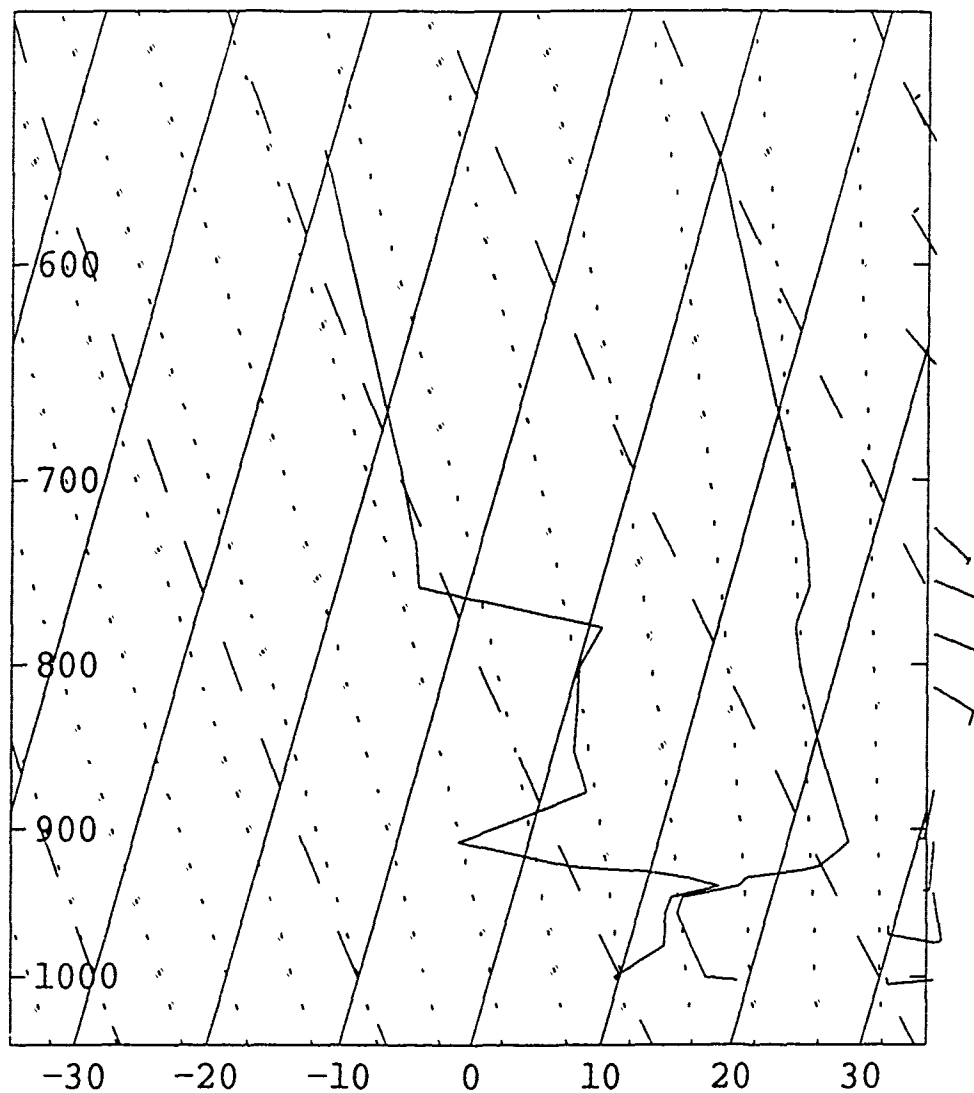
Figure 3.5. Skew T-Log P diagram for the 00 UTC, August 3, 1990 Vandenberg AFB sounding. Pressure is in mb, temperature and dew point temperature are in °C. Winds are shown using the standard station plotting convention.
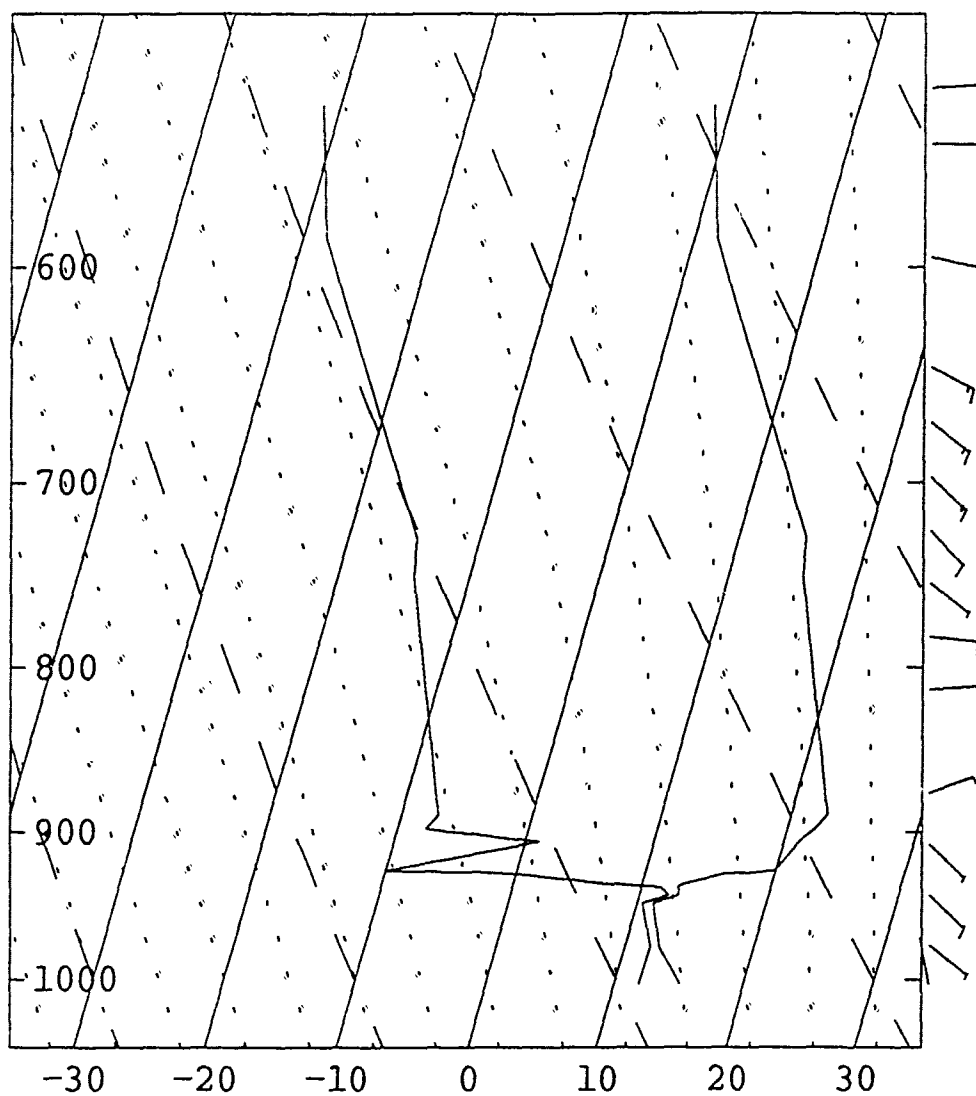
Figure 3.6. Skew T-Log P diagram for the 12 UTC, August 3, 1990 Vandenberg AFB sounding. Pressure is in mb, temperature and dew point temperature are in °C. Winds are shown using the standard station plotting convention.

Oakland. In terms of the diurnal changes in the structure and strength of the inversion, they are very similar.

A summary of the inversion characteristics for each of the soundings is compiled in Table 3.3. The definitions of the base and top of the inversion are the same as for the Oakland observations. The base of the inversion at Vandenberg AFB on 12 UTC August 2, 1990, is at a pressure level of 938 mb, where the temperature and relative humidity are 13°C and 96% respectively, while the top of the inversion is at a pressure level of 885 mb, where the temperature is 24°C and the relative humidity is 13%.

The largest magnitude of the refractivity gradient calculated by IREPS is 2215 N-units per km between the 933 mb and 932 mb pressure levels (Table 3.4). Also, between the 938 mb and 933 mb pressure levels, the relative humidity falls from 96% to 43%, giving a refractivity gradient magnitude of 872 N-units per km. At both of these levels, the refractivity gradient magnitude is well above the 157 N-units per km required for ducting, and it is interesting to note that if the temperatures were adjusted to their likely, higher values, then these gradients would be even stronger.

As noted above, the 00 UTC, August 3, 1990 sounding at Vandenberg AFB also appears to suffer from the evaporative cooling problem. In Figure 3.5, it is seen that the temperature begins to rise rapidly at 944 mb. At the same level, the dew point temperature would be expected to begin a significant fall as the air dries rapidly through the inversion. Instead, the radiosonde instruments show the dew point temperature rising up to the 937 mb pressure level. This may be an indication that there is some moisture accumulation on the radiosonde thermistor.

Table 3.3. Summary of the observed synoptic-scale subsidence inversion at Vandenberg AFB from the soundings in Figures 3.4, 3.5, and 3.6.

		Pressure	Temperature	Relative Humidity
		(mb)	(°C)	(%)
12 UTC	Base	938	13	96
August 2, 1990	Top	885	24	13
00 UTC	Base	944	13	95
August 3, 1990	Top	908	25	13
12 UTC	Base	941	13	95
August 3, 1990	Top	888	23	13

Table 3.4. Summary of the IREPS output calculated using the three observations at Vandenberg AFB given in Figures 3.4, 3.5, and 3.6. The pressure levels are those between which the refractivity gradient magnitude is the largest. The depth of the ducting layer is given by refractivity gradient magnitudes greater than 157 N-units per km.

	Pressure Levels	Maximum Refractivity Gradient Magnitude	Depth of Ducting Layer
	(mb)	(N-units/km)	(m)
12 UTC August 2, 1990	933-932	2215	438
00 UTC August 3, 1990	927-924	677	300
12 UTC August 3, 1990	926-925	1501	469

Again, the radiosonde data are accepted without any adjustment, and a summary of the inversion characteristics is compiled in Table 3.3. For this sounding, the base of the inversion is at a pressure level of 944 mb, with a temperature of 13°C and a relative humidity of 95%. The top of the inversion is at a pressure level of 908 mb, where the temperature is 25°C and the relative humidity is 13%. The temperature and relative humidity at both the base and top of the inversion are nearly the same for both soundings. However, the pressure level has increased by 8 mb at the base and 23 mb at the top of the inversion.

With very similar inversion base and top temperatures and relative humidities, it might be inferred that the ducting characteristics of the morning and afternoon soundings would also be similar. This is not the case, though, because surface heating and a sea breeze circulation combine to decrease the vertical moisture gradient during the day. Thus, the largest magnitude of the refractivity gradient calculated by the IREPS software for the 00 UTC, August 3, 1990 sounding is 677 N-units per km between 927 mb and 924 mb (Table 3.4). This gradient magnitude is substantially smaller than the 2215 N-units per km calculated from the 12 UTC, August 2, 1990 observation. Also, the thickness of the duct is 300 m, which is 138 m less than the thickness calculated for the morning sounding.

The Skew T-Log P diagram for the 12 UTC, August 3, 1990 Vandenberg AFB sounding is shown in Figure 3.6. As summarized in Table 3.3, the inversion base is at a pressure level of 941 mb, where the temperature is 13°C and the relative humidity is 95%. The inversion top is at a pressure level of 888 mb, where the temperature is 23°C and the relative humidity is 13%. Comparison of the characteristics of the inversion base and top at this hour with those seen 12 and 24 hours previously reveals that the temperature values are within 2°C and the humidity values are within 1%. The pressure levels of the base and top of the inversion have returned to values near those on 12 UTC, August 2, 1990.

The largest magnitude of the refractivity gradient for the 12 UTC, August 3, 1990 sounding is calculated by the IREPS software to be 1501 N-units per km between the 925 and 924 mb pressure levels (Table 3.4). This gradient magnitude is much larger than that calculated for the previous afternoon, but is somewhat smaller than that calculated for the previous

morning. Thus, for this sounding, the moisture gradient is not as steep as that observed at 12 UTC, August 2, 1990. However, the depth of the duct at 12 UTC, August 3, 1990 has returned to a value similar to that found 24 hours earlier.

As with the Oakland obser ations, surface heating and subsequent mixing of the moist marine boundary layer with dry air aloft has reduced the maximum refractivity gradient magnitude in the afternoon sounding. This process seems to be accompanied in this case by convergence aloft of northerly moving air that is deflected westward by the nearby Santa Ynez Mountains (Figure 2.3). Moisture is thus added to the atmosphere above the synoptic-scale subsidence inversion, thereby raising the top of the inversion layer in the morning soundings. Therefore, for Vandenberg AFB, neither the base nor the height of the inversion layer is constant, with the base rising over 230 m and the top rising 100 m between the morning and afternoon soundings. The thickness of the ducting layer decreases from 438 m in the morning to 300 m in the afternoon. Between the 00 UTC and 12 UTC, August 3, 1990 soundings, the strength of the subsidence inversion and the depth of the ducting layer return to values similar to those observed on 12 UTC, August 2, 1990. As found for the Oakland soundings, these changes in the inversion and ducting layers at Vandenberg AFB are consistent with expectations for diurnal variability in a location subject to the interactions of nearby terrain and a persistent marine boundary layer (Section 2.4).

3.2. Model Representation of Local Ducting Conditions

It is clear from the data presented in the previous section that the synoptic-scale subsidence inversion and its associated ducting conditions maintain their presence over these two stations. There are, however, significant diurnal changes in the structure of the inversion and its associated duct over both stations between the early morning and early evening data. Radiational cooling at night strengthens the subsidence inversion, while surface heating and mesoscale circulations during the day weaken it. The MM5 model must be capable of detecting these changes in the inversion between the morning data, which are represented at the initial and 24 hour times of this model run, and the early evening data, which are represented at the 12 hour time. A validation of the capabilities of the model in detecting the inversions is made by comparing the model output with the Oakland and Vandenberg AFB observations at the three times. It is expected that there will be significant model degradation of the inversion strength because of the 14 mb vertical resolution of the model at the altitudes of the inversion. Consequently, it is possible that the IREPS output might indicate only superrefractive conditions where ducting conditions actually exist.

3.2.1. Model Representation of Ducting at Oakland

The grid column of the model located nearest to Oakland has (x,y) coordinates of (14,46). At this location on 12 UTC, August 2, 1990, the model inversion base is located at a pressure level of 956 mb, where the model

temperature is 12°C, and the model relative humidity is 96% (Table 3.5). The top of the model inversion is at 899 mb, where the model temperature is 27°C, and the model relative humidity is 10%. From Table 3.5, it is clear that the model has represented the temperature and relative humidity very well at the base and top of the inversion. The pressure level of the model inversion base differs from the observation by only 8 mb, while the pressure level of the top of the inversion differs by 17 mb. With the 14 mb vertical grid resolution at these levels, the model values of the pressure levels for the base and top of the inversion are thus essentially within one vertical grid level of the observed values.

Within the modeled inversion, the largest magnitude of the model-based refractivity gradient, as calculated by the IREPS software, is 370 N-units per km, and is located between the 942 mb and 928 mb pressure levels (Table 3.6). In contrast, calculations from the sounding show this maximum refractivity gradient to be between 945 mb and 942 mb pressure levels, with magnitudes greater than that required for ducting extending to the 929 mb pressure level. Thus, all the pressure levels at which ducting conditions occurred in the observations were within one grid layer of the model.

That the model generates refractivity gradient magnitudes large enough to imply ducting conditions between these pressure levels shows that the model represents the altitudes of strongest ducting quite well, despite its 14 mb vertical resolution. Also, the model duct depth is within 4% of the depth of the duct calculated from the observations. These findings indicate that the model has captured the initial ducting conditions over Oakland as well as might be expected.

Table 3.5. Summary of the observed and modeled synoptic-scale subsidence inversions at Oakland for 12 UTC, August 2, 1990.

		Pressure (mb)	Temperature (°C)	Relative Humidity (%)
Observation	Base	948	12	95
	Top	916	28	14
Model	Base	956	12	96
	Top	899	27	10

Table 3.6. Comparison of the IREPS output calculated using observations and model data for Oakland on 12 UTC, August 2, 1990. The pressure levels are those between which the refractivity gradient magnitude is the largest. The depth of the ducting layer is given by refractivity gradient magnitudes greater than 157 N-units per km.

	Pressure Levels (mb)	Maximum Refractivity Gradient Magnitude (N-units/km)	Depth of Ducting Layer (m)
Observation	945-942	680	455
Model Output	942-928	370	470

At 00 UTC, August 3, 1990, the model had similar success in representing the inversion over Oakland (Table 3.7). The model inversion base is at a pressure level of 960 mb, with a temperature of 16°C and a relative humidity of 87%, and the model inversion top is at a pressure level of 883 mb, with a model temperature of 24°C, and a model relative humidity of 23%. The model temperature and relative humidity output for the base and top of the inversion compares favorably with the observations. The only significant deviation is in the pressure level of the top of the model inversion, which varies by more than two vertical grid layers from the observed pressure level.

Comparisons of the level of maximum refractivity gradient magnitude shows that there is good agreement between the model and the observation (Table 3.8). The maximum magnitude of the model refractivity gradient calculated by the IREPS software is between the 946 mb and 932 mb pressure levels, while the observations indicate the maximum refractivity gradient magnitude is between the 939 mb and 932 mb pressure levels. Unfortunately, despite the excellent representation of the level of maximum refractivity gradient magnitude by the MM5 model, its 14 mb vertical resolution leads to a decrease of the magnitude of the refractivity gradient to a value that is not greater than the 157 N-units per km required for ducting conditions. Thus, the IREPS software is unable to produce a ducting layer depth from the model data, although it at least indicates superrefraction.

The model continues to be successful in representing the subsidence inversion at Oakland on 12 UTC, August 3, 1990 (Table 3.9). The model inversion begins at a pressure level of 961 mb, where the model temperature

Table 3.7. Observed and modeled synoptic-scale subsidence inversion at Oakland for 00 UTC, August 3, 1990.

		Pressure	Temperature	Relative Humidity
		(mb)	(°C)	(%)
Observation	Base	955	16	81
	Top	915	26	22
Model	Base	960	16	87
	Top	883	24	23

Table 3.8. Summary of the IREPS output calculated using observations and model data for Oakland on 00 UTC, August 3, 1990. The pressure levels are those between which the refractivity gradient magnitude is the largest. The depth of the ducting layer is given by refractivity gradient magnitudes greater than 157 N-units per km.

	Pressure Levels	Maximum Refractivity Gradient Magnitude	Depth of Ducting Layer
	(mb)	(N-units/km)	(m)
Observation	939-932	360	187
Model Output	946-932	157	---

Table 3.9. Observed and modeled synoptic-scale subsidence inversion at Oakland for 12 UTC, August 3, 1990.

		Pressure (mb)	Temperature (°C)	Relative Humidity (%)
Observation	Base	948	12	95
	Top	916	26	13
Model	Base	961	13	96
	Top	883	24	14

is 13°C and the model relative humidity is 96%. The model pressure is within one vertical grid level, the temperature is within 1°C, and the relative humidity is within 1% of the observed values for the inversion base. The top of the model inversion is at a pressure level of 883 mb, where the model temperature is 24°C and the model relative humidity is 14%. These results compare very favorably with the observed pressure level, temperature, and relative humidity at the top of the inversion.

Comparisons of the modeled and observed maximum refractivity gradient magnitudes, as calculated by the IREPS software, are shown in Table 3.10. The model places the maximum refractivity gradient magnitude one grid level too high in altitude and weakens it considerably, and it underrepresents the depth of the ducting layer. However, the model still produces a maximum refractivity gradient magnitude greater than the 157

N-units per km critical value required for ducting conditions. The weakening of the duct is again caused primarily by the 14 mb vertical resolution at the altitude of the inversion.

Table 3.10. Comparison of the IREPS output calculated using observations and model data for Oakland on 12 UTC, August 3, 1990. The pressure levels define the layers in which the refractivity gradient magnitude is the largest. The depth of the ducting layer is given by refractivity gradient magnitudes greater than 157 N-units per km.

	Pressure Levels	Maximum Refractivity Gradient Magnitude	Depth of Ducting Layer
	(mb)	(N-units/km)	(m)
Observation	944-940	1281	476
Model Output	932-918	247	257

3.2.2. Model Representation of Ducting at Vandenberg AFB

The comparison between observations and model data for Vandenberg AFB uses the grid column with the (x,y) coordinate (26,17). The model initialization for 12 UTC, August 2, 1990 shows the model inversion base to be at a pressure level of 959 mb, with a model temperature of 14°C, and a model relative humidity of 92% (Table 3.11). The top of this model inversion is 859 mb, with a model temperature of 21°C, and a model relative humidity

Table 3.11. Observed and modeled synoptic-scale subsidence inversion at Vandenberg AFB on 12 UTC, August 2, 1990.

		Pressure	Temperature	Relative Humidity
		(mb)	(°C)	(%)
Observation	Base	938	13	96
	Top	885	24	13
Model	Base	959	14	92
	Top	859	21	17

of 17%. The comparison of the observations with the model output in Table 3.11 shows that the model does not handle the strength and thickness of the inversion at Vandenberg AFB as well as it handled them over Oakland. The model weakens the inversion at the base by raising the temperature and lowering the humidity. At the top of the inversion, the model weakens the inversion by lowering the temperature and raising the humidity. Also, the inversion layer is raised by 21 mb at the base and 26 mb at the top, so that the model inversion is more than three vertical grid layers too deep.

Despite the weakening, deepening, and lifting of the inversion by the model, it is nevertheless very successful at capturing the level of the largest magnitude of the refractivity gradient. As shown in Table 3.12, the largest observed refractivity gradient magnitudes are between the 933 mb and 932

Table 3.12. Comparison of the IREPS output calculated using observations and model data for Vandenberg AFB on 12 UTC, August 2, 1990. The pressure levels define layers in which the refractivity gradient magnitude is the largest. The depth of the ducting layer is given by refractivity gradient magnitudes greater than 157 N-units per km.

	Pressure Levels	Maximum Refractivity Gradient Magnitude	Depth of Ducting Layer
	(mb)	(N-units/km)	(m)
Observation	933-932	2215	438
Model Output	945-931	163	140

mb pressure levels. The IREPS software, using model output, calculates the largest gradient to be between the 945 mb and 931 mb pressure levels. As with the Oakland case, the model has placed the level of the maximum refractivity gradient magnitude in the correct grid layer. However, the weakening of the refractivity gradients due to the 14 mb vertical resolution of the model appears to have greatly reduced the magnitude of the maximum refractivity gradient and the depth of the ducting layer. The observed value of the maximum refractivity gradient magnitude is 13 times greater than the model-based one, and the depth of the ducting layer calculated from the observations is three times greater than that calculated from model output. Thus, at Vandenberg AFB, the model initialization is very good in reproducing the level of the maximum refractivity gradient, but less

successful in representing the strength of the refractivity gradient and the depth of the ducting layer.

The model representation of the inversion over Vandenberg AFB does not improve significantly at the 12-hour time of the model run, although the model does represent correctly the trends in the observed values between the two observations. Table 3.13 shows a comparison of the 00 UTC, August 3, 1990 observations with the model output. Once again, the model weakens the inversion at the base and top, with the relative humidity being 13% too low at the base and 13% too high at the top of the inversion. The error in the pressure level of the base has decreased to 4 mb at the top of the inversion, but is still more than two vertical grid layers too low at the base. Thus, despite weakening and vertically broadening the inversion, the model does follow the trend of lowering the altitude of the inversion base and raising the altitude of the inversion top (Tables 3.11 and 3.13).

The IREPS software, using model output, calculates the height of the maximum model refractivity gradient magnitude to be within one vertical grid layer of the observed value (Table 3.14). The observed data show the maximum refractivity gradient magnitude to be between the 927 mb and 924 mb pressure levels, while the model output shows the maximum gradient magnitude to be between the 948 mb and 934 mb pressure levels (Table 3.14). Like the Oakland case for 00 UTC, August 3, 1990, the magnitude of the maximum gradient of refractivity calculated from model output does not exceed the critical 157 N-units per km required for ducting conditions. Thus, there is no ducting layer depth to be calculated for the model output. Once again, the 14 mb vertical resolution of the model weakens the refractivity,

Table 3.13. Observed and modeled synoptic-scale subsidence inversions at Vandenberg AFB on 00 UTC, August 3, 1990.

		Pressure (mb)	Temperature (°C)	Relative Humidity (%)
Observation	Base	944	13	95
	Top	908	25	13
Model	Base	976	17	82
	Top	904	22	26

Table 3.14. Comparison of the IREPS output calculated using observations and model data for Vandenberg on 00 UTC, August 3, 1990. The pressure levels define the layers in which the refractivity gradient magnitude is the largest. The depth of the ducting layer is given by refractivity gradient magnitudes greater than 157 N-units per km.

	Pressure Levels (mb)	Maximum Refractivity Gradient Magnitude (N-units/km)	Depth of Ducting Layer (m)
Observation	927-924	677	300
Model Output	948-934	130	---

which greatly affects the ability of the IREPS software to deliver an accurate representation of ducting conditions.

The model representation of the inversion is better at the 24 hour time than it is at the 12 hour time (Table 3.15). The base of the model inversion is at a pressure level of 977 mb, where the model temperature is 14°C and the model relative humidity is 91%. The top of the model inversion is at a pressure level of 904 mb, where the model temperature is 22°C and the model relative humidity is 16%. The model inversion base and top are significantly lower in altitude than the observed inversion base and top. However, the model inversion base and top temperatures are within 1°C and the relative humidities are within 4% of the observed values.

The representation of the maximum refractivity gradient magnitude by the model is too low in altitude (Table 3.16). In this case, though, the error is only one vertical grid layer, as found for previous soundings. The maximum model refractivity gradient magnitude is calculated by IREPS to be 265 N-units per km between the 948 and 934 mb pressure levels. The observed maximum refractivity gradient magnitude is 1501 N-units per km between the 926 and 925 mb pressure levels. As with all previous comparisons, the coarse 14 mb vertical resolution of MM5 at the altitude of the inversion weakens the refractivity gradient magnitude significantly.

3.2.3. Model Representation of Single Station Ducting Conditions

In summary, a comparison of model output with observations shows that the model representation of the synoptic-scale subsidence inversion is

Table 3.15. Observed and modeled synoptic-scale subsidence inversions at Vandenberg AFB on 12 UTC, August 3, 1990.

		Pressure	Temperature	Relative Humidity
		(mb)	(°C)	(%)
Observation	Base	941	13	95
	Top	888	23	13
Model	Base	977	14	91
	Top	904	22	16

Table 3.16. Comparison of the IREPS output calculated using observations and model data for Vandenberg on 12 UTC, August 3, 1990. The pressure levels define the layers in which the refractivity gradient magnitude is the largest. The depth of the ducting layer is given by refractivity gradient magnitudes greater than 157 N-units per km.

	Pressure Levels	Maximum Refractivity Gradient Magnitude	Depth of Ducting Layer
	(mb)	(N-units/km)	(m)
Observation	926-925	1501	469
Model Output	948-934	265	257

limited by the relatively coarse 14 mb resolution of the model at the altitude of the subsidence inversion (Figure 3.7). However, the model represents well the trends in the depth of the inversion at both locations. The model output, through the IREPS software calculations, is especially successful in representing the level of the maximum refractivity gradient magnitude in all six comparisons. However, refractivity gradients calculated by the IREPS program from both model soundings at the 12 hour time of the model run, at 00 UTC August 3, 1990 do not exceed the critical threshold for ducting conditions, although ducting is indicated from the observations at both stations.

The vertical resolution of the model in the vicinity of the inversion ensures that the actual refractivity gradient magnitudes must be at least as great, and likely greater than the model-derived refractivity gradient magnitudes. Thus the region of maximum values of the refractivity gradient magnitude are more important than the 157 N-unit per km critical value for ducting. Also, it can be noted that anywhere that the model predicts ducting conditions is unambiguous since it has been shown above that the resolution of the model decreases the strength of the duct in all cases. Thus it is seen that although the 14 mb vertical resolution of the model at the altitude of the synoptic-scale subsidence inversion causes it to underestimate the maximum refractivity gradient magnitudes and to deepen the inversion in all cases with respect to the observations. The model does appear to do well in representing both the trends in the evolution of the inversion characteristics and the height of the maximum refractivity gradient magnitude.
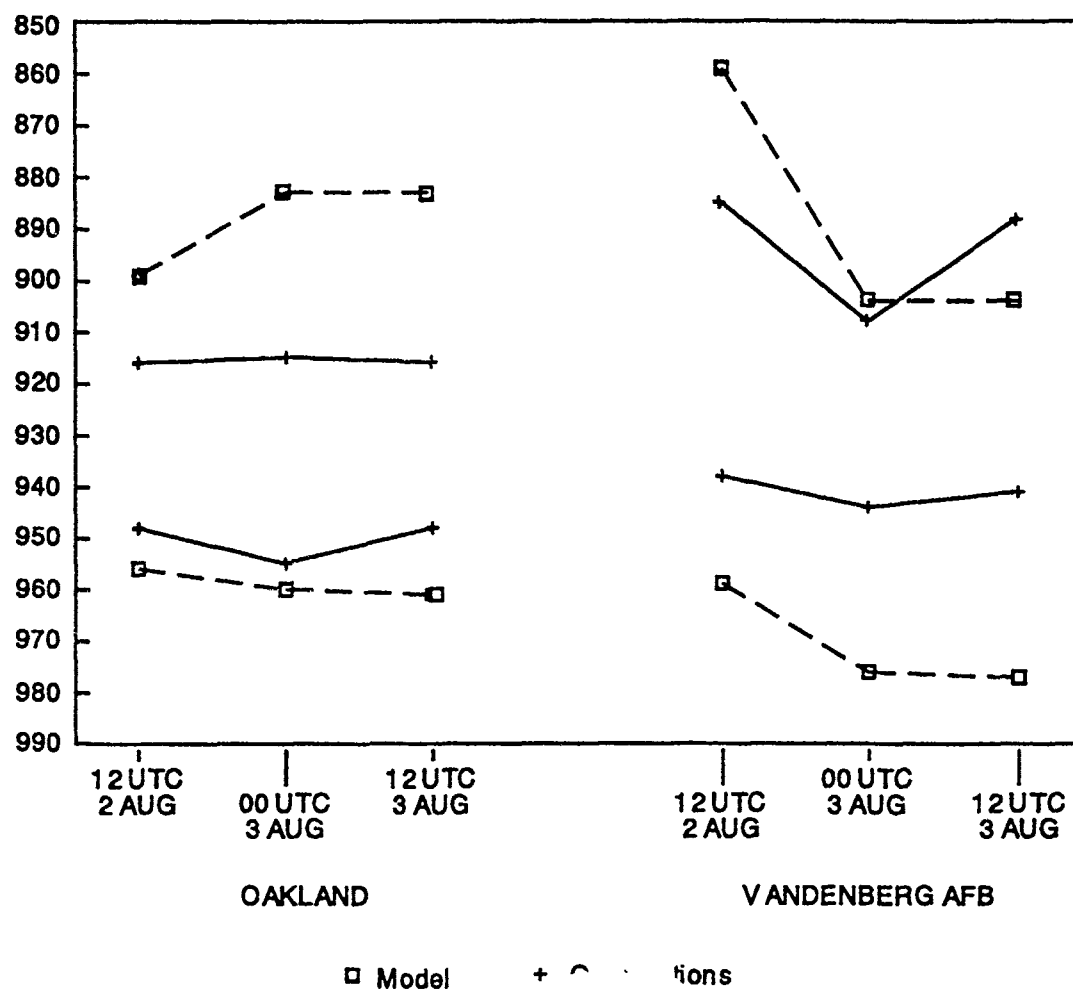
55

Figure 3.7. Observed and modeled inversion base and top pressure levels for Oakland and Vandenberg AFB on 12 UTC, August 2, 1990, and 00 and 12 UTC, August 3, 1990. Pressure levels are in mb.

3.3. Model Representation of Regional Ducting Conditions

It has been shown in Section 3.2 that the MM5 model can capture qualitatively the trends in the inversion depths and the magnitudes of the maximum refractivity gradients. Having thus calibrated the performance of the model within two grid columns, an examination of the spatial variations of inversion and ducting strength can be made using the MM5 model and IREPS. To accomplish this, temperature and relative humidity data at every other grid point in the model for 12 UTC August 2, 1990, and 00 and 12 UTC, August 3, 1990 were assembled for the area spanning ten grid points east and west of Oakland and ten grid points east and west of Vandenberg AFB. Then, for each grid point, the model data were entered into the IREPS program, and the resulting maximum refractivity gradient magnitude was plotted. Finally, contouring of the data allowed a determination of the ducting regime behavior over the area.

3.3.1. Spatial Ducting Characteristics for 12 UTC, August 2, 1990

For the MM5 model initial time, 12 UTC. st 2, 1990, most of the west-central California area would be expected have some ducting conditions, either at the surface or aloft. The areas in which ducting would not be expected are those that are above the altitude of the moist boundary layer at which the decrease in moisture aloft was insufficient to cause ducting conditions. Within the general area in which ducting conditions are present, there would be a refractivity gradient magnitude maximum expected along the coast, where radiational cooling and local circulations might

combine with the synoptic-scale subsidence inversion to produce enhanced ducting conditions.

Figure 3.8 shows the model-derived spatial variation in the maximum refractivity gradient magnitudes for the 12 UTC, August 2, 1990 initial time. The most notable feature of the contour plot is the strong horizontal gradient in the maximum vertical refractivity gradient magnitude along the north coast. This occurs because an area of stratocumulus capping the marine boundary layer provides a strong, sharp temperature and moisture gradient at the top of the layer where it is bounded by the dry air above.

To the south, though, there is a notable decrease in the maximum refractivity gradient magnitudes, particularly over the water. This may be an area in which the model produces a poor representation of vertical moisture gradients and stratocumulus clouds. The decrease in the representativeness of the model between Oakland and Vandenberg AFB gives reason to suspect that the north-south horizontal gradient of the maximum vertical refractivity gradient magnitude is artificial. It is noted, however, that there is a tongue of relatively stronger gradients extending southward along the coast. This extension is likely the result of a land breeze circulation and radiational cooling combining to provide a local intensification of the vertical moisture and temperature gradients (Section 2.4).

Inland and east of the Coastal Range, values of the maximum refractivity gradient are lower than they are along the coast because there is less moisture present in the atmosphere. However, the combination of subsidence and radiational cooling concentrates what moisture is available near the surface, resulting in the presence of some ducting conditions in the Central Valley.

Figure 3.8. Model-derived spatial variation in the maximum refractivity gradient magnitudes for 12 UTC, August 2, 1990. Contours are in N-units per km. Areas in which ducting conditions occur are shaded, with darker shading indicating regions of greater duct strength.

Thus it is shown that although the model seems to have poor representation over the water, it can capture the expected horizontal variations in the maximum vertical refractivity gradient magnitudes along the coast and inland. As discussed in section 2.3, these variations are the result of the interactions between synoptic-scale and mesoscale weather systems.

3.3.2. Spatial Ducting Characteristics for 00 UTC, August 3, 1990

The situation at the 12 hour time of the model run, 00 UTC, August 3, 1990, is much more interesting because strong surface heating of the land mass has significantly altered the pattern of the refractivity gradient magnitude maxima. From Figure 3.9, it is clear that the strongest ducting conditions are now on the western slopes of the Coastal Range. Meanwhile, the dry Central Valley has been heated significantly during the day, resulting in a mountain-valley circulation. Hot and dry Central Valley air flows up the east side of the Coastal Range, providing little moisture, and hence, no refractivity gradients conducive to ducting over this area. When the air reaches the peaks of the range, some of the air returns over the valley. However, some of the hot dry air cascades westward over the Coastal Range, intensifying the cap of the inversion, thereby providing maximum daytime values of the refractivity gradient magnitude there.

Over the water, a significant decrease in the refractivity gradient magnitude maxima is evident. This would imply that there is a significant decrease in the coverage of the stratocumulus layer along the coast and overthe water. However, surface observations along the coast show that the
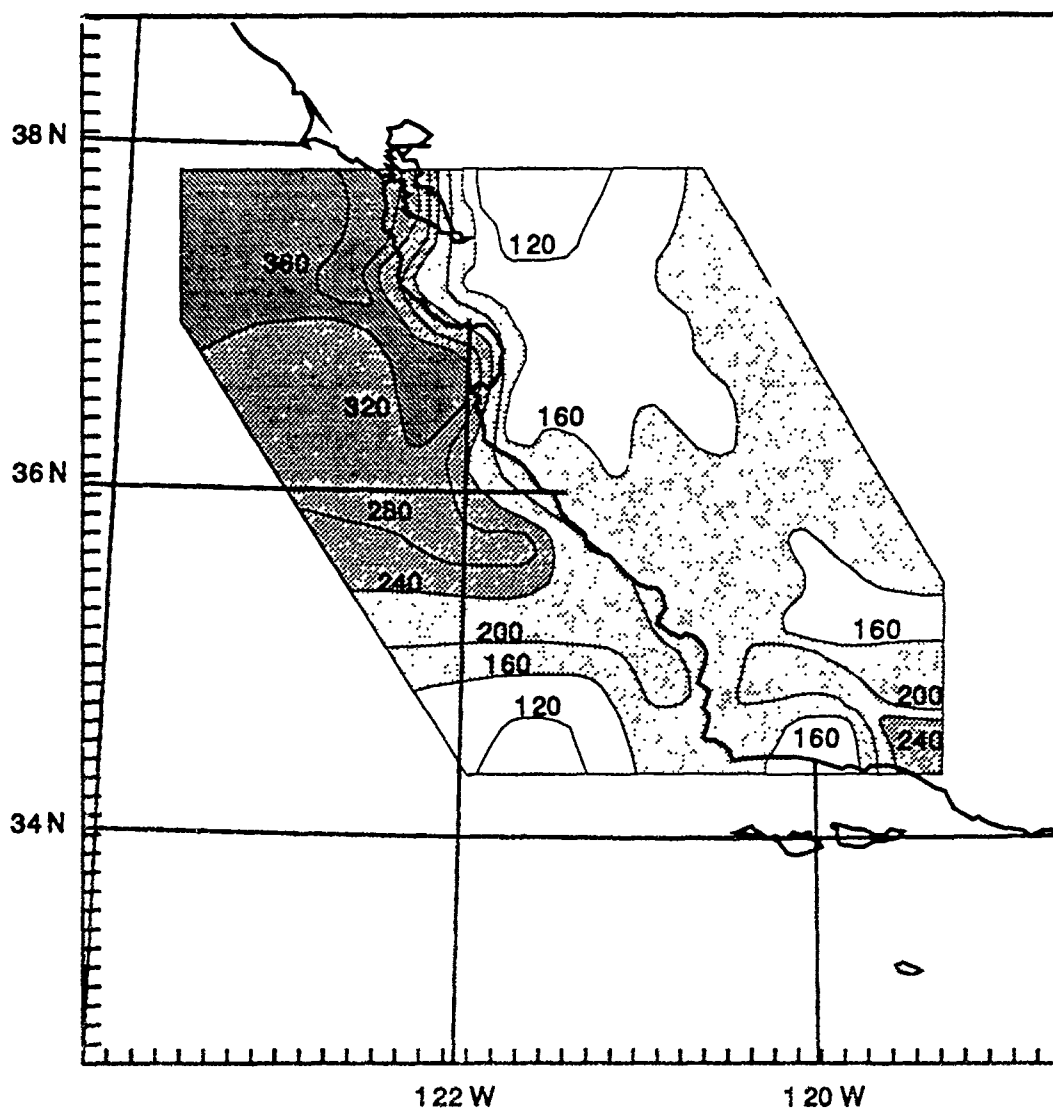
Figure 3.9. Model-derived spatial variation in the maximum refractivity gradient magnitudes for 00 UTC, August 3, 1990. Contours are in N-units per km. Areas in which ducting conditions occur are shaded, with darker shading indicating regions of greater duct strength.

layer was present during the mornings of August 2-3, 1990. Figure 3.10 also shows that the stratocumulus layer was widespread offshore during the evening of August 3, 1990. Thus, the relatively low values of the maximum vertical refractivity gradient magnitudes calculated from the model output over the water suggests that marine stratocumulus clouds are not well simulated by the model.

3.3.3. Spatial Ducting Characteristics for 12 UTC, August 3, 1990

The effects of terrain and synoptic-scale and local circulations on the spatial ducting characteristics of the west-central California land areas are seen in Figure 3.11. The prevailing synoptic-scale flow near the surface is from the northwest. This flow provides a continuous stream of cool and moist marine air. A combination of land breeze and mountain valley circulations cause a localized easterly flow down the northwest and west slopes of the Coastal ranges. This localized flow is warm and dry, and it should have the effect of intensifying the subsidence inversion at these locations. The model represents this condition well, with local maxima in the refractivity gradient magnitudes along the northwest and west slopes of all the ranges. Along the ridges, subsidence is enhanced by the land breeze and mountain valley circulation return flows. However, there is no moisture available there to create the strong refractivity gradient magnitudes necessary for ducting conditions.

Over the Central Valley, the ducting regime is dependent on terrain and geographic location. Again, the mountain valley circulation should enhance the subsidence inversion and refractivity gradient magnitudes along
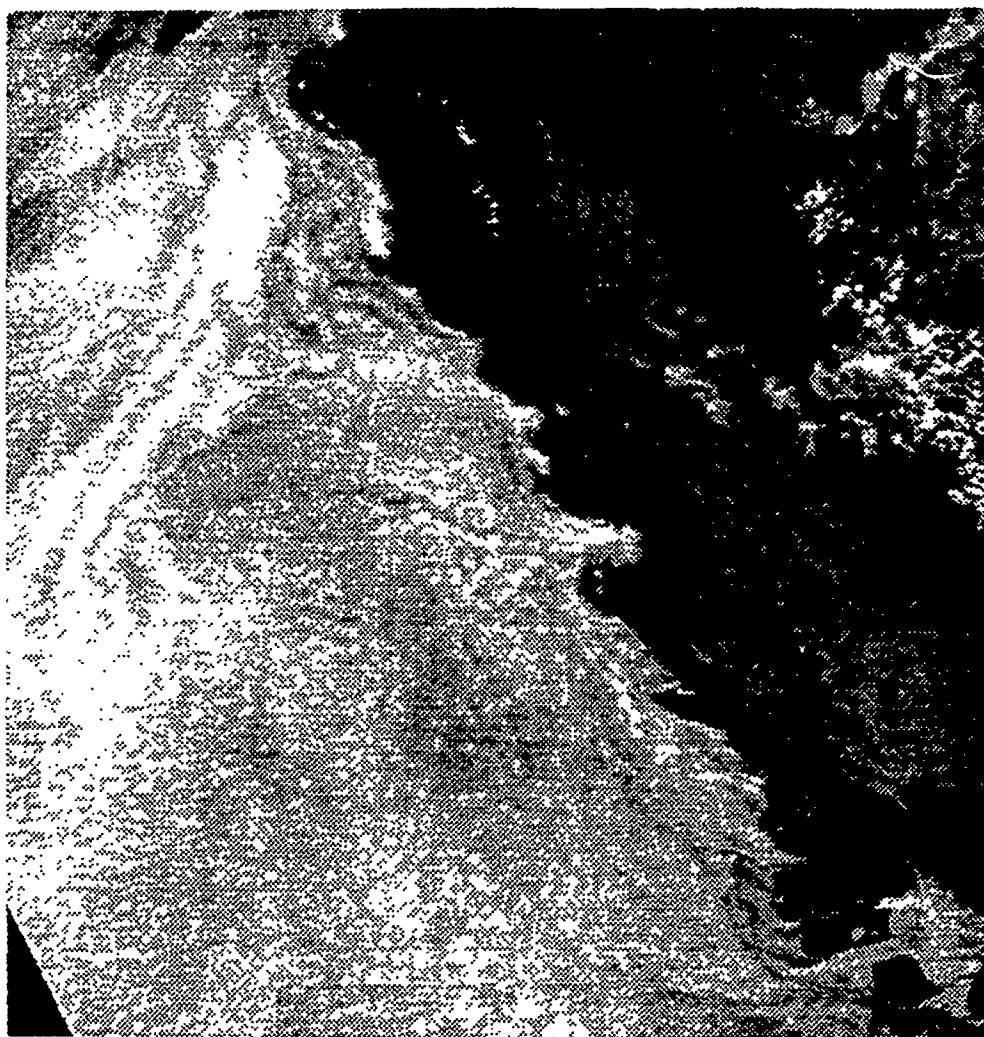
Figure 3.10. Visible image of the Pacific coast taken from an AVHRR polar-orbiting satellite at 21 UTC, August 3, 1990. An extensive area of stratocumulus clouds was located just off the California coast.
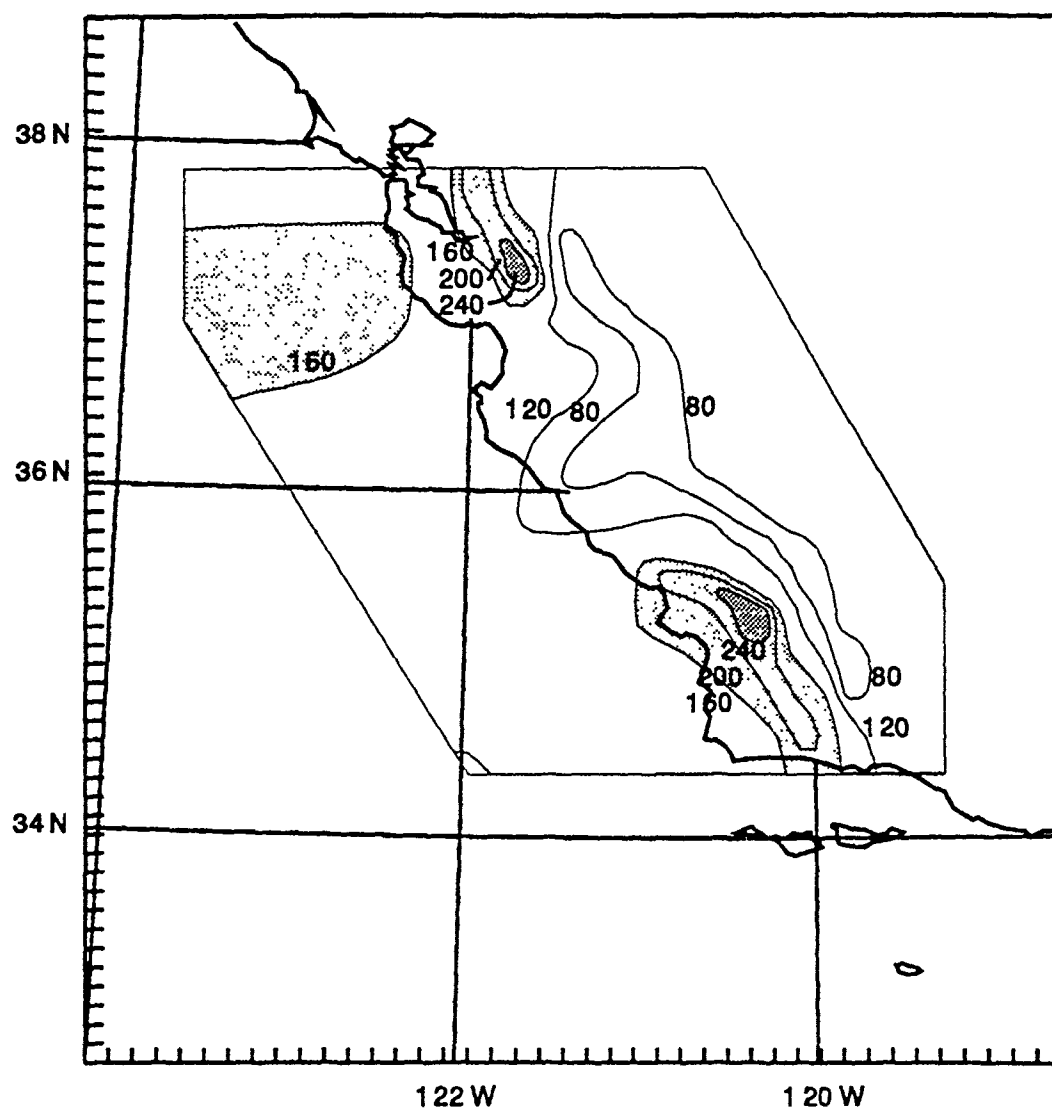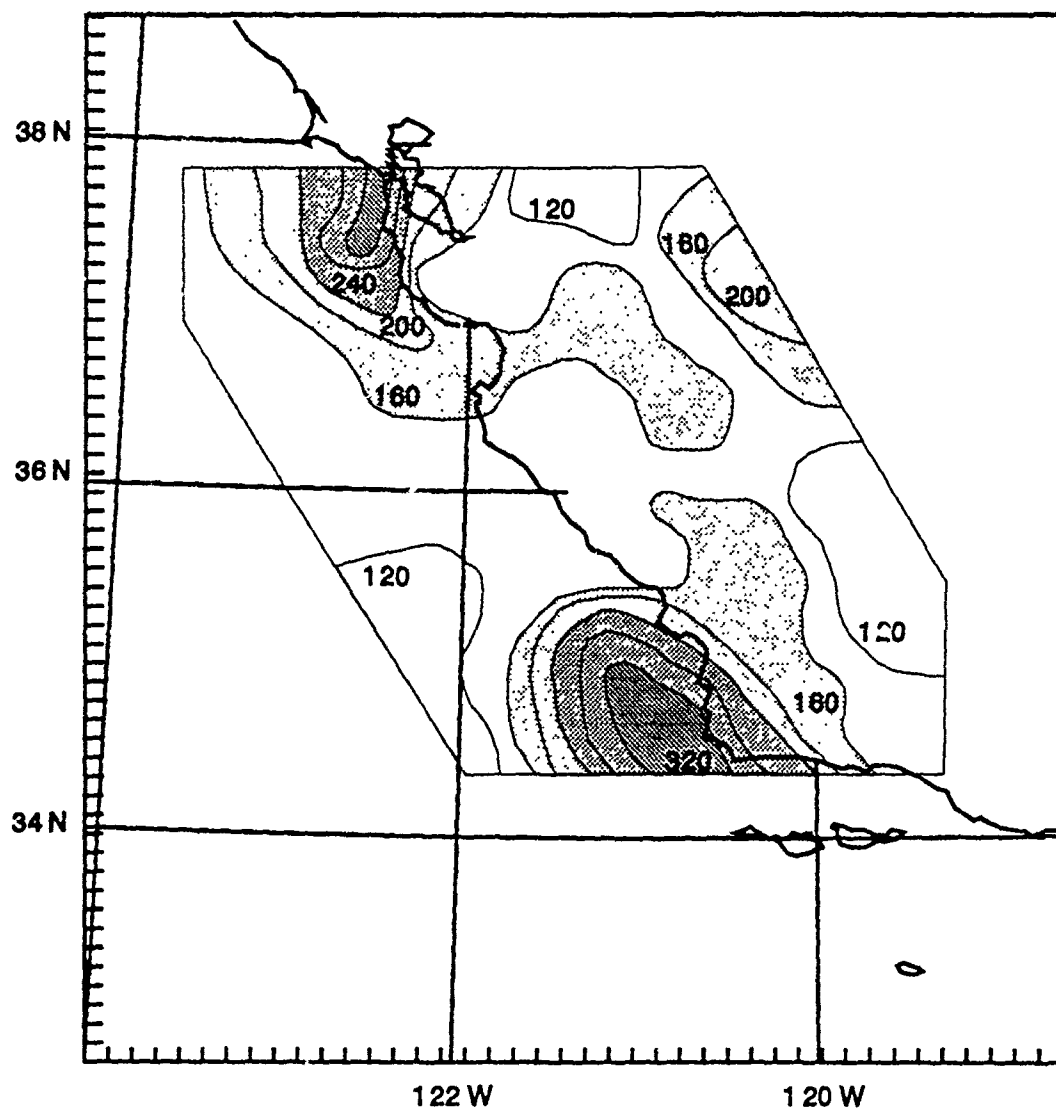
Figure 3.11. Model-derived spatial variation in the maximum refractivity gradient magnitudes for 12 UTC, August 3, 1990. Contours are in N-units per km. Areas in which ducting conditions occur are shaded, with darker shading indicating regions of greater duct strength.

the slopes of the mountains and degrade the subsidence inversion over the valley floor. However, ducting conditions are highly dependent on vertical gradients of moisture. Over the southern portion of the valley, there is not enough moisture to generate ducting conditions despite strong subsidence along the slopes of the Coastal Range. Over the central and northern portions of the Central Valley, there is an enhancement of refractivity gradient magnitude along the slopes of both the Coastal Range and the Sierra Nevada, and there is a degradation of refractivity gradient magnitudes on the valley floor.

Over the Pacific Ocean, it would be expected that the subsidence inversion and the presence of stratocumulus capping the boundary layer would create refractivity gradient magnitudes large enough to generate ducting conditions. However, the model is unable to capture the expected gradients for several reasons. As stated previously, the 14 mb vertical resolution at the top of the subsidence inversion artificially weakens the moisture and temperature gradients. Also, the model suffers from a lack of data over the Pacific Ocean, preventing an accurate assessment of conditions by the model. Finally, the vertical diffusion schemes used in the model may be too strong, weakering the large gradients in temperature and moisture that occur at the top of the subsidence inversion.

3.4 Conclusion

The presere of a synoptic-scale subsidence inversion over west-central California during the August 2-3, 1990 period produced ducting conditions of

varying strength over the area. The MM5 model successfully reproduced the inversion over Oakland and Vandenberg AFB. The model also proved to be successful in reproducing the height of the maximum refractivity gradient magnitude and the trends in the inversion depth at the two locations. Spatially, the model represented expected trends in the horizontal gradients of the maximum vertical refractivity gradient magnitudes over coastal and inland areas. However, the 14 mb vertical resolution of the model at the inversion level and the seemingly poor representation of marine stratocumulus over the water led to a significant underrepresentation of ducting conditions, especially over the Pacific Ocean.

Chapter 4

CONCLUSIONS AND RECOMMENDATIONS FOR FURTHER STUDY

Atmospheric ducting of electromagnetic waves is a form of anomalous propagation that is a result of strong vertical gradients of moisture and temperature in the lower troposphere. This ducting can have significant effects on radar coverage. Within a duct, radar range can increase dramatically. Above the duct, however, there can be a large area in which there is a radar hole. Aircraft flying within a radar hole will not be detected by the radar. One of the major causes of large-scale atmospheric ducting of electromagnetic waves is a subsidence inversion.

A subsidence inversion is a semi-permanent feature over west-central California during the summer, and was present during the August 2-3, 1990 period. This thesis examines a means for improving current operational ducting forecasts by 1) examining the utility of the MM5 mesoscale model in representing the subsidence inversion in two grid columns, and 2) using model output to diagnose regional ducting conditions through the application of the Navy's IREPS single-station ducting analysis software.

The model was successful in representing the subsidence inversion over Oakland, and moderately successful over Vandenberg AFB. Model output entered into the IREPS software revealed that model ducting conditions were weaker than actual ducting conditions at the initial and 24-

hour forecast time, and they were too weak to diagnose ducting conditions in the two grid columns at 12 hours. This weakening seemed to be primarily the consequence of the 14 mb vertical resolution in the model near the altitude of the inversion. Despite the weakening of the inversion, though, the model represented regional trends in the expected ducting conditions over inland areas well. Over water, however, an apparent deficiency in the MM5 parameterization of marine stratocumulus weakened the subsidence inversion and ducting conditions more than would be expected between the initial and 12-hour forecast times and maintained this weakness at the 24-hour forecast time.

Further research in this area should include improving the vertical resolution of MM5, devising new parameterizations for marine stratocumulus, integrating MM5 and IREPS output directly into radar algorithms, and finding more efficient methods of displaying regional ducting conditions.

4.1. Current Operational Duct Forecasting Methods

To emphasize the importance of the mesoscale model to forecasts of ducting conditions, it is important to consider the current state of operational ducting forecasts at U.S. Air Force weather units. Most forecasters have only rudimentary knowledge of the causes and effects of atmospheric ducting. Consequently, IREPS output, if provided at all, is given to pilots with little input from forecasters, and with little knowledge about the temporal and horizontal inhomogeneities of ducting conditions. Thus, in cases such as the one presented in this thesis, conditions over Oakland and Vandenberg would

likely be linearly interpolated in order to determine ducting conditions between the two stations.

For example, the 12 UTC, August 2, 1990 soundings from Oakland and Vandenberg AFB might be entered into the IREPS software to obtain a ducting analysis. The output for each station, shown in Tables 3.2 and 3.4 respectively, would be used in a briefing to provide the current ducting conditions. Two important, but incorrect assumptions would most likely be made concerning the temporal and spatial variation in ducting conditions. The first assumption would be that the ducting conditions would remain constant over time. The second assumption would be that the ducting level would increase in altitude linearly from north to south, and that the thickness of the duct would remain uniform. However, the IREPS output from the 00 UTC, August 3, 1990 soundings (Tables 3.2 and 3.4) contradict the first assumption, and Figures 3.7 and 3.8 show that the second assumption is also incorrect.

Temporal and spatial variations in atmospheric ducting conditions are thus seen to be extremely complex. As demonstrated in this thesis, the combination of a mesoscale model and the IREPS software together provide important improvements in the forecasting of these variations.

4.2. Model Effectiveness in Duct Forecasting

As discussed in Chapter 3, the model effectively reproduced inversion conditions over Oakland and Vandenberg AFB at the initial, 12, and 24 hour times of the model. At Oakland, the model correctly represented the inversion base and top temperatures within 2°C, and relative humidities

within 6%. At Vandenberg AFB, the temperature spread was 4°C, and the relative humidities were both within 13% of the observed values. The input of model data into IREPS shows better representation of ducting conditions over Oakland as well. The model also correctly reproduced expected trends in the subsidence inversion at both locations, and it was very successful in representing the height of the maximum refractivity gradient magnitude at both locations. However, the 14 mb vertical resolution of MM5 near the altitude of the subsidence inversion decreased the model refractivity gradient magnitudes to less than the critical value for ducting (157 N-units per kilometer) at both locations for the 12-hour time of the model.

The effectiveness of MM5 in representing expected ducting conditions over the entire west-central California region was best over the land areas. An expected horizontal maximum in the vertical refractivity gradient magnitude was found along the coastline at the initial time of the model. At 12 hours, the model reproduced the expected maxima in the refractivity gradient magnitudes along the west slope of the Coastal Range, and minima along the east slopes. Over the Central Valley, MM5 correctly reflected the expected decreases in the maximum refractivity gradient magnitudes between the initial and 12 hour times. Over water, however, the magnitudes of the refractivity gradients fell too much between the initial and 12-hour times. This fall may reflect the inadequate parameterizations of marine stratocumulus by MM5.

Thus, the two greatest problems noted in the model are the 14 mb resolution near the level of the subsidence inversion and the inadequate representation of marine stratocumulus. Improving the resolution of MM5 is a simple, but costly solution to the first problem. The additional

computations required to double or triple the number of levels in the model would not be difficult, but would substantially increase the time and expense in running the model. In contrast, the problems encountered in the parameterization of marine stratocumulus are a well known deficiency in mesoscale models. To obtain any sort of predictability of ducting conditions over water, these parameterizations must be improved sufficiently that the strong moisture and temperature gradients can be detected near the stratocumulus layer. Until this is completed, little improvement in the forecasting of ducting conditions over the water will be made.

4.3. Applications of Findings

The mesoscale model is effective in capturing trends in the height and magnitudes of the maximum refractivity gradients. For some atmospheric ducts close to the ground, there can be significant consequences for aircraft detection capability. Below the duct, ground-based radars will have extended ranges, but may give inaccurate range information. Just above the duct, aircraft will be in the radar hole, and will not be detected by radar. Thus, in order for radar controllers to get an accurate picture of the range of an aircraft, it must be at least several hundreds of meters above the duct, depending on its distance from the ground radar. This is important in the case of small civilian aircraft that are not equipped with transponders. With the guidance in duct height and strength provided by a model like MM5, a controller would be aware of any limitations in radar detection capabilities owing to the presence of atmospheric ducts. For pilots interested in avoiding

detection by ground radar, MM5 output combined with appropriate computer guidance could produce the best flight path and altitude for detection avoidance.

4.4. Recommendations for Further Research

Undoubtedly, continuation of the trends in computer speed and memory capabilities will help to alleviate the layer resolution problems in MM5. A sharpening of the vertical resolution to 5 mb or less would vastly improve the capability of MM5 to accurately represent inversion and ducting conditions. In addition, the critical value of the refractivity gradient magnitude necessary for atmospheric ducting, 157 N-units per km, must be altered to apply to a mesoscale model since this critical value is based on a derivative, not a finite difference. A sensitivity study could be conducted that would determine how the critical value of the refractivity gradient magnitude would change with vertical grid resolution.

The problem of marine stratocumulus representation in mesoscale models has been recognized, and research continues in this area through field programs such as FIRE (Albrecht et al. 1988) and ASTEX. As noted above, improvements in this area are critical, because the strong vertical gradients of moisture at the top of the marine boundary layer are one of the primary causes of atmospheric ducts.

Integration of ducting analysis and forecasting software into radar algorithms would increase the accuracy of information displayed to the controller. Current systems use the standard atmosphere to calibrate equipment and to determine refractivity effects. A field experiment could be

conducted to verify the spatial and temporal variability of ducting conditions. Then, ducting analysis and forecasting software could be integrated into radar algorithms to greatly reduce radar range and height errors for all types of atmospheric conditions.

Perhaps the most critical area for further research is the development of a more effective means of displaying ducting information. The IREPS software produces only a two-dimensional ducting analysis. It is easy to imagine the visualization of ducting conditions expanded to include three spatial dimensions and time by combining IREPS with a mesoscale model. This would give radar controllers, pilots, and military commanders a clear picture of the effects of atmospheric ducting on radar coverage.

REFERENCES

Albrecht, B., D. Randall, and S. Nicholls, 1988: Observations of Marine Stratocumulus Clouds During FIRE, *Bull. Am. Met. Soc., 69*, 618-626.

Bean, B. R., and E.J. Dutton, 1968: *Radio Meteorology*, Dover Publications, Inc., New York, 258 pp.

Dotson, M.E., 1987: An Evaluation of the Impact of Variable Temporal and Spatial Data Resolution upon IREPS, Master's Thesis, Naval Postgraduate School, Monterey, California, 58 pp.

Felsch, P., and W. Whitlatch, 1990: Stratus Surge Prediction Along the Central California Coast, NOAA Tech. Mem. NWS WR-209, U.S. Dept. of Commerce, Washington, D.C, 17pp.

Garratt, J.R., and W.L. Physick, 1985: The Inland Boundary Layer at Low Latitudes: II Sea Breeze Influences, *Bound.-Layer Meteor., 33*, 209-231.

Holton, J.R., 1977: *An Inroduction to Dynamic Meteorology*, Academic Press, Inc., New York, 391 pp.

Hornbeck, D., 1983: *California Patterns; A Geographical and Historical Atlas*, Mayfield Publishing Co.,Palo Alto,California,117 pp.

Kessler, R.C., and S.G. Douglas, 1991: A Numerical Study of Mesoscale Eddy Development Over the Santa Barbara Channel, *J. Appl. Meteor., 30*, 633-651.

Mass, C.F., M.D. Albright, and D.J. Brees, 1986: The Onshore Surge of Marine Air into the Pacific Northwest: A Coastal Region of Complex Terrain, *Mon.Wea. Rev., 115*, 2602-2627.

Mass, C.F., and M.D. Albright, 1987: Coastal Southerlies an Alongshore Surges of the West Coast of North America: Evidence of Mesoscale Topographically Trapped Response to Synoptic Forcing, *Mon.Wea. Rev., 115*, 1707-1737.

McIlveen, R., 1986: *Basic Meteorology*, Van Nostrand Reinhold, Berkshire, England, 457 pp.

Nash, J., and F. Schmidlin, 1987: WMO international Radiosonde Comparison Final Report: Instrument and Observing Methods, World Meteorological Organization, Geneva, 103pp.

Patterson, W.L., 1988: Effective Use of the Electromagnetic Products of TESS and IREPS, Naval Ocean Systems Center, San Diego, 138pp.

Patterson, W.L., 1990: Integrated Refractive Effects Prediction System (IREPS) User's Manual, Naval Ocean Systems Center, San Diego, 39pp.

Schmidlin, F.J., 1988: WMO International Radiosonde Intercomparison, Phase II, 1985, NASA Goddard Space Flight Center, Wallops Island, Virginia,113 pp.

Seaman, N., D. Stauffer, and T. Tesche, 1992: The SARMAP Meteorological Model: A Four-Dimensional Data Assimilation Technique Used to Simulate Mesobeta-Scale Meteorology During a Hish Ozone Episode in California, AWMA Conference on Tropospheric Ozone Nonattainment and Design Values, Boston, Oct. 27-30.